Activation of the cation channel TRPM3 in perivascular nerves induces vasodilation of resistance arteries

Lucía Alonso-Carbajo[1,2], Yeranddy A. Alpizar[1], Justyna B. Startek[1], José Ramón López-López[2], María Teresa Pérez-García[2] and Karel Talavera[1]

[1] Department of Cellular and Molecular Medicine, Laboratory of Ion Channel Research, KU Leuven; VIB Center for Brain & Disease Research, Herestraat 49, Campus Gasthuisberg, O&N1 Box 802, 3000 Leuven, Belgium.

[2] Departamento de Bioquímica y Biología Molecular y Fisiología, Instituto de Biología y Genética Molecular, Universidad de Valladolid y CSIC, Sanz y Forés 3, 47003 Valladolid, Spain.

Address correspondence to:

Prof. Dr. Karel Talavera

Laboratory of Ion Channel Research

Dept. of Cellular and Molecular Medicine, KU Leuven

Herestraat 49, Campus Gasthuisberg, O&N1 Box 802

B-3000 Leuven, Belgium

Phone: +32 16 330 469

Fax: +32 16 330 732

Email: karel.talavera@kuleuven.vib.be

Abstract

The Transient Receptor Potential Melastatin 3 (TRPM3) is a Ca^{2+}-permeable non-selective cation channel activated by the neurosteroid pregnenolone sulfate (PS). This compound was previously shown to contract mouse aorta by activating TRPM3 in vascular smooth muscle cells (VSMC), and proposed as therapeutic modulator of vascular functions. However, PS effects and the role of TRPM3 in resistance arteries remain unknown. Thus, we aimed at determining the localization and physiological role of TRPM3 in mouse mesenteric arteries. Real-time qPCR experiments, anatomical localization using immunofluorescence microscopy and patch-clamp recordings in isolated VSMC showed that TRPM3 expression in mesenteric arteries is restricted to perivascular nerves. Pressure myography experiments in wild type (WT) mouse arteries showed that PS vasodilates with a concentration-dependence that was best fit by two Hill components (effective concentrations, EC_{50}, of 14 and 100 μM). The low EC_{50} component was absent in preparations from *Trpm3* knockout (KO) mice and in WT arteries in the presence of the CGRP receptor antagonist BIBN 4096. TRPM3-dependent vasodilation was unaffected by the β-adrenergic antagonist propranolol, but was partially inhibited by a cocktail of K^+ channel blockers. We conclude that, contrary to what was found in aorta, PS dilates mesenteric arteries, partly via an activation of TRPM3 that triggers CGRP release from perivascular nerve endings and a subsequent activation of K^+ channels in VSMC. We propose that TRPM3 is implicated in the regulation of the tone of resistance arteries and that its activation by yet unidentified endogenous damage-associated molecules lead to protective vasodilation responses in mesenteric arteries.

Keywords: TRPM3; perivascular nerve; vasodilation; pregnenolone sulfate; CGRP

Nonstandard Abbreviations and Acronyms:

AC	Adenylate cyclase
α-SMA	Alpha-smooth muscle actin
β-gal	β-galactosidase
cAMP	cyclic adenosine monophosphate
CGRP	Calcitonin gene-related peptide
EC	Endothelial cells
GAPDH	Glyceraldehyde 3-phosphate dehydrogenase
HEK293T	Human embryonic kidney cell 293 SV40 T-antigen
KO	Knockout
NA	Noradrenaline
NF-200	Neurofilament 200
PGP9.5	Protein gene product 9.5
PKA	Protein kinase A
PS	Pregnenolone sulfate
SMDS	Smooth muscle dissociation solution
TH	Tyrosine Hydroxylase
TRP	Transient Receptor Potential
TRPM	Transient Receptor Potential Melastatin
UTP	Uridine-5′-triphosphate
VSMC	Vascular smooth muscle cells

1. Introduction

Several members of the Transient Receptor Potential (TRP) protein superfamily have been recently identified in vascular smooth muscle, endothelial and perivascular cells, and their study is an emerging theme in cardiovascular research [1, 2]. TRP proteins form cation channels, and with the exceptions of TRPM4 and TRPM5, all of them permeate Ca^{2+} [3]. TRP channel activation can thus directly affect Ca^{2+}-dependent signaling and modulate the membrane potential, and thereby the function of voltage-gated K^+ and Ca^{2+} channels that ultimately determine the vascular tone. There are substantial discrepancies about TRP channel functions in the vascular system, most of which arise from the lack of appropriate pharmacological tools and the difficulty of studying these channels in native cellular conditions [2]. Yet, several TRP channels have been implicated in the regulation of the vascular tone via multiple mechanisms. For instance, TRPC channels were identified as receptor-operated or store-operated Ca^{2+} entry channels in vascular smooth muscle cells (VSMC) [4, 5], activation of TRPV4 in VSMC and endothelial cells (EC) induces vasodilation [6, 7], and TRPV1 and TRPA1 contribute to vasodilation mediated by stimulation of perivascular sensory nerves [8, 9].

The role of the melastatin family of TRP channels (8 members, TRPM1 to TRPM8) in vascular function remains ill-defined in most cases. TRPM4 has been shown to participate in the myogenic response of cerebral arteries [10], but seems to be absent in other resistance arteries [11]. TRPM2 is expressed in EC and regulates endothelial permeability [12], while TRPM6 and TRPM7 have been found in VSMC as critically involved in Mg^{2+} homeostasis [13]. Regarding TRPM3 [14-16], it has only recently been described mRNA and protein expression in mouse aorta and human saphenous

89 veins [17]. Activation of TRPM3 by the steroid pregnenolone sulfate (PS) was reported
90 to induce aortic contraction, as deduced from the inhibitory effects of antibodies
91 blocking this channel. However, multiple key questions on the role of TRPM3 to
92 vascular function remain open. First, the specificity of PS as TRPM3 agonist in vascular
93 tissue has not been tested with the use of *Trpm3* knockout (KO) mice. Second, the
94 contributions of TRPM3 to the tone of resistance arteries and to the regulation of blood
95 pressure are still unknown. Recent findings unveiling TRPM3 as thermo-sensor and
96 potential chemo-sensor in nociceptive neurons [18, 19] suggest that, if present in
97 perivascular nerve endings, activation of this channel might result in neuropeptide
98 release. This would suppose a vasodilating effect of TRPM3 activation, an action
99 opposite to the vasoconstriction previously described in mouse aorta [17].

100 In order to address these questions, we first investigated the localization of TRPM3 in
101 mouse mesenteric arteries. Next, we performed myography experiments in arteries
102 isolated from wild type (WT) and *Trpm3* KO mice to determine the specificity of PS
103 and to characterize the mechanism of action of this compound. We found that, contrary
104 to what was reported for aorta [17], PS induces vasodilation of mesenteric arteries, and
105 that these effects are partly mediated by activation of TRPM3, via release of CGRP and
106 subsequent activation of K^+ channels in VSMC. Our data support a contribution of
107 TRPM3 as a potential therapeutic target for the modulation of the tone of resistance
108 arteries and as a plausible effector of endogenous damage-associated molecules
109 mediating protective responses in these vascular beds.

110

111

2. Methods

2.1 Mice

The experiments were performed on WT C57bl/6J (Janvier Laboratories, Saint-Berthevin Cedex, France) and *Trpm3* KO male mice weighing about 25 g and from 10-12 weeks of age. They received standard food and drinking water *ad libitum*. Animals were anesthetized and then euthanized by CO_2 inhalation. The *Trpm3* KO mice are global knockouts produced by the insertion of a cassette containing a beta-geo fusion construct flanked by a 5'-terminal IRES sequence into exon 17 of the mouse *Trpm3* gene by homologous recombination [19, 20]. These mice have a decreased sensitivity to heat [19], but are otherwise viable, fertile, and exhibit no differences from WT animals in terms of general appearance and gross anatomy. All protocols were in accordance with the European Community and Belgian Governmental guidelines for the use and care of experimental animals (2010/63/EU, CE Off Jn8L358, LA12110551) and approved by the KU Leuven Ethical Committee Laboratory Animals (ECD) and the Institutional Care and Use Committee of the University of Valladolid.

2.2 Isolation of VSMC

Segments of third-order mesenteric arteries were dissected and cleaned of adipose tissue in cold oxygenated smooth muscle dissociation solution (SMDS) containing (in mM): 145 NaCl, 4.2 KCl, 0.6 KH_2PO_4, 1.2 $MgCl_2$, 10 HEPES, glucose 11 (pH 7.4, adjusted with NaOH) and 10 Ca^{2+}. The dissected arteries were subjected to two consecutive processes of enzymatic digestion in order to isolate VSMC. The first digestion was carried out at 37 °C for 14-16 min in SMDS-Ca^{2+}-free solution containing 0.8 mg/ml papain (Worthington Biochemical Corp.), 1 mg/ml BSA (Sigma-Aldrich) and 1 mg/ml

dithiothreitol (Sigma-Aldrich). The second digestion was performed at 37 °C for 14-16 min using SMDS-10 μM Ca^{2+} supplemented with 0.6 mg/ml collagenase F (Sigma-Aldrich) and 1 mg/ml BSA. Digested arteries were rinsed twice with SMDS-10 μM Ca^{2+}. After this washing step, single cells were obtained by mechanical disruption with a wide-bore glass pipette. Cells were maintained at 4 °C until they were used in patch-clamp recordings.

2.3 qRT – PCR analyses

Mesenteric arteries were enzymatically digested as described in the previous section, but decreasing the incubation time to 8-10 min with the enzymes and skipping the washing step with SMDS-10 μM Ca^{2+}, so that nerve fibers, smooth muscle and endothelial cells were still present in the preparation. Arteries of 6 mice were used for each determination. Total RNA from the digested arteries was extracted using RNeasy mini kit (Qiagen), following the manufacturer's protocol. cDNA synthesis was performed with 500 ng of total RNA of the previous step using Ready-to-go First strand beads (GE Healthcare). A small fraction of the cDNAs was used for quantitative real-time PCR. Each qPCR reaction (20 μl) contained 3 μl of cDNA template, 10 μl of Universal TaqMan MasterMix (2x concentrated, Life Technologies), 1 μl of TaqMan probe (Table 1, 20x concentrated, Life Technologies) and 6 μl H_2O. For every experiment, test reactions were performed in triplicate, and non-template negative controls in duplicate. Fluorescent signals generated during PCR amplifications were normalized to an internal reference (GAPDH). The threshold cycle (Ct) was set within the exponential phase, and the relative quantitative evaluation of target gene levels was performed using the $2^{-\Delta Ct}$ method. Differences between samples with and without endothelium were calculated as $2^{-\Delta\Delta Ct}$, where $\Delta\Delta Ct = \Delta Ct_{without} - \Delta Ct_{with}$.

Gene Name	Assay ID	GenBank mRNA	Exon boundary	Assay location	Amplicon length
TRPM1	Mm00450619	AF047714.1	6 - 7	822	90
TRPM2	Mm00663098	AB166747.1	29 - 30	4265	107
TRPM3	Mm00616485	AK051867.1	21 - 22	3135	75
TRPM4	Mm00613173	AJ575814.1	9 - 10	1204	78
TRPM5	Mm00498453	AB039952.1	18 - 19	2787	73
TRPM6	*Mm00463112*	AK080899.1	13 - 14	1520	125
TRPM7	Mm00457998	AY032951.1	13 - 14	1752	125
TRPM8	Mm00454566	AF481480.2	24 - 25	3389	89
GAPDH	4352932E	NM008084.2	--	--	107

Table 1. List of TRP-specific TaqMan gene expression assays (Life Technologies).

2.4 Immunofluorescence microscopy

Intact arteries were fixed with 4% paraformaldehyde (PFA) in PBS for 15 min, permeabilized in PBTx (PBS, 0.2% Triton X-100) and blocked with PBTx with 2% of sheep serum for 3 h. Arteries were incubated overnight at 4 °C with the primary rabbit anti-TRPM3 (1:100, Santa Cruz), mouse anti-NF-200 (1:1000, Alomone), human anti-PGP9.5 (1:100, Santa Cruz), chicken anti-β-gal IgY (1:1000, Abcam), rabbit anti-calcitonin gene-related peptide (1:500, Abcam), mouse anti-tyrosine hydroxylase (1:1000, Abcam) or rabbit anti-alpha smooth muscle actin (1:250, Abcam) antibodies, followed by the secondary antibodies Alexa 594 goat anti-rabbit (1:1000, Molecular Probes), Alexa 555 anti-mouse (1:1000, Abcam), 488 donkey anti-chicken or goat anti-chicken IgY-Alexa 488 (1:1000, Abcam). Secondary antibodies were prepared in blocking solution and incubated for at least 2 h at room temperature. Finally, the arteries were flat-mounted in glass slides using DAPI-containing mounting solution (VectaShield, Vector Laboratories).

HEK293T cells were plated in polyL-lysine-coated coverslips, fixed with 4% PFA in PBS for 15 min and blocked with PBS with 2% of sheep serum for 3 h. The cells were incubated with primary antibody rabbit anti-TRPM3 (1:100, Santa Cruz) overnight at 4 °C. After that, samples were incubated with the secondary antibody Alexa 594 goat anti-rabbit (1:1000, Molecular Probes) in blocking solution during 2 h at 22 °C. The coverslips were mounted using DAPI-containing mounting solution (VectaShield, Vector Laboratories).

Confocal images of labeled cells and arteries were collected using the optimal pinhole size for the Plan-Apochromat 63x/1.4 oil objective and 20x or 40x objective of a Zeiss LSM 510 Meta Multiphoton microscope (Carl Zeiss AG). Images were acquired by consecutive excitation with an Argon laser at 488 nm and He-Ne laser at 543 nm. For nuclear DAPI staining, we used a two-photon pulsed excitation by the Spectra-Physics (Mountain View) Mai Tai laser at 770 nm. Images were analyzed using ImageJ processing software.

2.5 Patch-clamp electrophysiology

Whole-cell patch-clamp recordings were performed in freshly isolated VSMC at ~22 °C using an Axopatch 200 patch-clamp amplifier (Axon Instruments, Molecular Devices), filtering at 2 kHz (-3 dB, four-pole Bessel filter), and sampling at 10 kHz. Recordings were digitized with a Digidata 1322A interface, driven by CLAMPEX 10 (Axon Instruments). Patch pipettes were made from borosilicate glass (2.0 mm O.D., WPI) and double pulled (Narishige PP-83) to resistances ranging from 2 to 5 MΩ when filled with the internal solution. For K_V channel recordings, the composition of this solution was (in mM): 125 KCl, 4 $MgCl_2$, 10 HEPES, 10 EGTA, 5 Mg^{2+}-ATP, pH 7.2 with KOH. The composition of the bath solution was (in mM): 141 NaCl, 4.7 KCl, 1.2 $MgCl_2$, 1.8

199 $CaCl_2$, 10 glucose and 10 HEPES, pH 7.4 with NaOH. The voltage dependence of K^+
200 currents were obtained applying 200 ms pulses from a holding potential of -80 mV to
201 voltages between -60 to +60 mV in 20 mV steps, at a frequency of 5 s. Whole-cell
202 patch-clamp recordings of TRPM3 currents were carried out with solutions of the
203 following composition (in mM): 141 NaCl, 1.8 $CaCl_2$, 1.2 $MgCl_2$, 5 CsCl, 10 glucose,
204 10 HEPES, 0.005 nicardipine, 0.1 DIDS and 0.1 niflumic acid (pH 7.4 with NaOH) for
205 the extracellular solution and 10 CsCl, 110 Cs aspartate, 10 NaCl, 3.2 $CaCl_2$, 10
206 HEPES, 10 BAPTA, 2 Mg^{2+}-ATP (pH 7.2, adjusted with CsOH) and with an estimated
207 free [Ca^{2+}] of 100 nM for the intracellular solution. To determine the effects of PS (10
208 μM and 30 μM), CIM0216 (2 μM) and Uridine-5′-triphosphate (UTP, 100 μM) currents
209 were recorded upon stimulation with 1 s voltage ramps from -150 mV to +80 mV
210 applied from a holding potential of -10 mV, at a frequency of 5 s. Electrophysiological
211 data analyses were performed with the Clampfit subroutine of pCLAMP (Axon
212 Instruments) and with Origin 7.5 (OriginLab Corp.).

213 **2.6 Pressure myography experiments**

214 Third order mesenteric arteries were dissected and mounted in a myograph (Danish
215 Myo Technology 110P) that allowed controlling the luminal pressure while measuring
216 external arterial diameter via digital video edge detection (CCD camera). Artery
217 segments were cannulated between two borosilicate glass pipettes and fixed with nylon
218 filaments at both ends. The artery segments were filled with physiological saline
219 solution containing (mM): 120 NaCl, 2.5 $CaCl_2$, 1.17 $MgSO_4$, 5 KCl, 1.18 Na_2HPO_4, 25
220 $NaHCO_3$, 1 EDTA, 10 glucose (pH 7.4, adjusted with 5% CO_2–95% air, which was
221 maintained throughout the duration of the experiment) and were pressurized to 70
222 mmHg and allowed to stabilize at 37 °C for at least 15 min before starting the

measurements. Unless otherwise stated the artery segments were air-bubbled though the lumen to remove endothelial cells. Phenylephrine (10 μM) or noradrenaline (NA, 20 μM) was perfused to contract the arteries prior to the application of test compounds. PS and CIM were washed after their last application with physiological saline solution containing 10 μM phenylephrine. The data were analyzed using MyoView software. At the end of each experiment, we applied the L-type Ca^{2+} channel blocker nifepidine (10 μM) to determine the maximum arterial diameter. Nifedipine was previously reported as a TRPM3 agonist [21]. Thus, it could be argued that nifedipine-induced vasodilation may be partly mediated by TRPM3, making this compound unsuitable for the determination of the role of this channel. To test this, we compared the vasodilation elicited in the same artery by 10 μM nifedipine application and by perfusion with Ca^{2+}-free bath solution. We observed similar increase in the arterial diameter in both cases (Fig. S1). This demonstrates that 10 μM of nifedipine has the same effect than abrogating Ca^{2+} entry through L-type Ca^{2+} channels, thus validating its use to determine the maximal vasodilation. Vasodilation was determined using the formula 100 x (Dx - DPhe) / (DNif - DPhe). Dx, DPhe and DNif were the diameters recorded in the presence of PS and phenylephrine, phenylephrine alone and nifedipine, respectively. The resulting dose-response curves for PS were fitted using either one or two Hill functions of the forms:

$$Vasodilation\ (in\ \%) = 100\frac{[PS]^n}{[PS]^n + k^n}$$

were *[PS]*, n and k are the PS concentration, the Hill coefficient and the effective concentration, respectively, and:

$$Vasodilation\ (in\ \%) = 100\left(\frac{A_1[PS]^{n1}}{[PS]^{n1} + k_1^{n1}} + \frac{(1 - A_1)[PS]^{n2}}{[PS]^{n2} + k_2^{n2}}\right)$$

where A_1, $n1$ and k_1 are the relative amplitude, the Hill coefficient and the effective concentration of the first Hill component, respectively, and $n2$ and k_2 are the Hill coefficient and the effective concentration of the second Hill component, respectively. A maximum of two arteries was taken from each mouse. In those cases, the data was averaged.

2.7 Intracellular Ca^{2+} imaging

Ca^{2+} imaging experiments were conducted using the fluorescent indicator Fura-2AM. HEK293T cells stably expressing murine TRPM3 were cultured as previously described [19]. They were incubated with 5 μM Fura-2AM (Invitrogen) for 30 min at 37 °C. Fluorescence measurements were performed with a Zeiss Axioskop FS upright microscope fitted with an ORCA ER charge-coupled device camera. Fura-2AM was excited at 340 and 380 nm with a rapid switching monochromator (TILL Photonics). Mean fluorescence intensity ratios (F340/F380) were displayed online with Metafluor software (Molecular Devices).

2.8 Reagents

Pregnenolone sulfate, noradrenaline, propranolol and nifedipine were purchased from Sigma-Aldrich. CIM0216 was obtained from Prof. Joris Vriens. The CGRP receptor antagonist BIBN 4096 was obtained from Tocris Bioscience. K_V channel toxin blockers were purchased from Alomone Laboratories, and correolide was a gift from María García.

2.9 Statistical analyses

In all experiments, data were pooled from multiple trials carried out on cells or arteries isolated from at least three different animals and summarized as means ± SEM. The Origin software (version 8.6, OriginLab) was used for statistical analysis and data display. Differences between means were assessed using t-test paired or unpaired and one-way ANOVA, Dunn-Sidak test comparisons. $P < 0.05$ was taken as statistically significant difference between means.

3. Results

3.1 Expression pattern of TRPM family in mouse mesenteric arteries

We first determined the expression of the genes encoding TRPM channels in WT mouse mesenteric arteries with and without endothelium. *Trpm1*, *Trpm5* and *Trpm8* could not be detected after 40 cycles of amplification in any preparation. In contrast, the other 5 members of the subfamily were detected in preparations with endothelium (Fig. 1A). We found lower relative expression for *Trpm4* and *Trpm7* and no detectable *Trpm2* and *Trpm6* in preparations devoid of endothelium (Fig. 1A, B), suggesting for a preferential expression of these transcripts in the endothelial layer. In sharp contrast, we found higher relative levels of *Trpm3* mRNA in endothelium-free preparations, indicating for a predominant expression in the medial and/or adventitial layers. Of note, we found a much higher relative abundance of *Trpm3* mRNA in aorta than in mesenteric arteries (3.3 ± 0.8; $n = 3$ versus 0.09 ± 0.01; $n = 3$; $P < 0.001$; data not shown).

3.2 Localization of TRPM3 in perivascular nerves of mouse mesenteric arteries

Confocal images of mesenteric arteries labeled with the neuronal markers PGP9.5 (Fig. 1C) and neurofilament (NF-200; Fig. S2A) evidenced the presence of nerve fibers in the adventitial layer, but not in the smooth muscle layer (Fig. S2B). The localization of

TRPM3 was determined with an antibody whose specificity against TRPM3 was confirmed in a HEK293T cell line stably transfected with this channel (Fig. S3). As control for the experiment, we used TRPM5-transfected HEK293T cells, which also express TRPM7 endogenously [22]. We found that these cells were not stained with the anti-TRPM3 antibody, confirming the specificity for TRPM3 versus these closely-related TRPM channels (Fig. S3). We found that TRPM3 colocalized with PGP9.5 (Fig. 1C) and was absent in cells of the tunica media (VSMC), which were clearly identified by the distinct orientation of their nuclei, perpendicular to the axis of the vessel (Fig. 1D).

Of note, arteries from *Trpm3* KO mice could not be used as a negative control for the TRPM3 antibody, because these animals express a truncated TRPM3 protein that can be recognized by the anti-TRPM3 antibody. However, we took advantage of the fact that these mice have incorporated a β-galactosidase (β-gal) reporter encoded by the insertion of a *Lac-Z* gene into the reading frame of the *Trpm3* gene [20]. Using an anti-β-gal antibody in *Trpm3* KO mice, we found that β-gal colocalized with the neuronal markers PGP9.5 (Fig. 2A) and NF-200 (Fig. S2A) and was absent in VSMC (Fig. S2B). As expected for negative control, WT arteries were not stained with the anti-β-gal antibody (Fig. 2B). To further characterize the localization pattern of TRPM3 we performed double immunostaining in intact mesenteric arteries from *Trpm3* KO mice labeled with antibodies against β-gal and the smooth muscle-specific protein alpha-smooth muscle actin (α-SMA). We found α-SMA to be present as expected in the smooth muscle (Fig. 3A), but not in the adventitial layer (Fig. 3B). In contrast, β-gal was clearly detected only in nerve ending-like structures in the adventitial layer.

To test directly whether TRPM3 is functionally expressed in the medial layer of mouse mesenteric arteries we performed whole-cell patch-clamp recordings in freshly dissociated VSMC. Application of PS (10 and 30 μM) produced no significant change in the current amplitude at -80 mV and +150 mV (99.9 ± 0.5% and 100 ± 0.3% relative to the amplitude recorded in control condition, respectively; n = 12 cells from 4 mice; Fig. 4A). In another series of experiments, the effects of PS (10 μM) and of the potent TRPM3 synthetic agonist CIM0216 [18] on current amplitude were compared to the effects of the purinergic receptor agonist UTP [23]. Again, there was no change in current amplitude during PS application (-0.3 ± 0.3 pA, P = 0.95, at -150 mV and 1.3 ± 0.9 pA, P = 0.77 at +80 mV (n = 6 cells from 3 mice; Fig. 4B, black trace in right panel). Currents were also unaffected by 2 μM CIM0216 (current amplitude change of -0.5 ± 1.7 pA, P = 0.99 at -150 mV and 2 ± 2 pA, P = 0.77 at +80 mV; n = 4 cells from 2 mice; Fig. 4C, black trace in right panel). On the other hand, currents were stimulated at negative potentials by 100 μM UTP, as expected. The amplitude of the UTP-sensitive current was -51 ± 9 pA, P = 0.003 at -150 mV and 2.7 ± 0.7 pA, P = 0.26 at +80 mV; n = 5 cells from 2 mice (Fig. 4B, C, grey traces in right panels). Taken together, these data indicate the absence of functional expression of TRPM3 channels in mesenteric arteries VSMCs.

3.3 TRPM3 activation induces vasodilation mainly via stimulation of CGRP receptors

To determine the effects of TRPM3 activation in resistance arteries we performed pressure myography experiments in endothelium-denuded mouse mesenteric arteries. Pressurized arteries were pre-contracted with 10 μM phenylephrine to maintain the physiological tone. PS induced a dose-dependent reversible vasodilation in arteries

dissected from WT animals. The data was best fit by the sum of two Hill functions, suggesting for at least two targets of PS (Fig. 5A, D). The EC_{50} values for these components were 14 ± 2 μM and 100 ± 9 μM and the corresponding Hill coefficients (*H*) were 2.2 ± 0.5 and 4.3 ± 1.2, respectively. This fitting also yielded a value of relative amplitude of the low EC_{50} vasodilation component of 57 ± 7% (A_1, see the two-Hill components equation in the Methods, section Pressure myography experiments). To determine the contribution of TRPM3 channels to the effects of PS we measured the response of mesenteric arteries isolated from *Trpm3* KO mice. PS dilated *Trpm3* KO arteries only at concentrations higher than ~10 μM (Fig. 5B, D). The dose-response curve for *Trpm3* KO arteries could be fitted with a single Hill function, with EC_{50} and Hill values of 53 ± 3 μM and 2.2 ± 0.2, respectively. These results further support the idea that in WT arteries there are two different mechanisms involved in PS-induced vasodilation, being only the one with lower EC_{50} TRPM3-dependent. Also, CIM0216 induced a dose-dependent reversible vasodilation in arteries from WT animals, with EC_{50} and Hill coefficients values of 0.40 ± 0.05 μM and 0.65 ± 0.06, respectively (Fig. S4A, C). Arteries dissected from *Trpm3* KO mice responded to this compound, but at concentrations higher than 0.1 μM, with EC_{50} and Hill coefficients values of 1.50 ± 0.08 μM and 1.6 ± 0.1, respectively (Fig. S4B, C).

Based on prior studies on sensory TRP channels such as TRPV1 and TRPA1 [8, 9] and the expression of TRPM3 in nociceptive neurons [18, 19], as well as the well-stablished neuroanatomical localization of CGRP in perivascular nerves innervating the adventitial layer [24-27], we hypothesized that the TRPM3-dependent vasodilation induced by PS may be mediated by the release of CGRP and the relaxing effect of this peptide on VSMC. To test this, we performed myography experiments in the presence of the CGRP receptor antagonist BIBN 4096. In this condition, PS-induced vasodilation could

only be elicited at concentrations above 10-15 μM (Fig. 5C). The dose-response curve of the effect of PS in the presence of BIBN 4096 was similar to the curve obtained in arteries from *Trpm3* KO mice, with EC_{50} and H values of 44 ± 2 μM and 1.8 ± 0.1, respectively (Fig. 5D). Furthermore, double immunolabelling of intact mesenteric arteries from *Trpm3* KO mice with anti-β-gal and anti-CGRP antibodies showed a good colocalization in the sensory fibers that innervate the adventitial layer (Fig. 5E). These results indicate that TRPM3 location seems to be restricted to sensory nerve endings, where the TRPM3-mediated effect of PS depends on CGRP receptor activation.

The vasodilating action of CGRP has endothelium-dependent and endothelium-independent components, which are mediated by the stimulation of CGRP receptors in endothelial cells and VSMC, respectively [28, 29]. Thus, the TRPM3-dependent effect of PS is expected to be stronger in the presence of endothelium. We found that this was indeed the case, as PS induced a dose-dependent biphasic effect in intact arteries (Fig. S5A), with EC_{50} values lower than the corresponding ones found in endothelium-denuded preparations (8.1 ± 0.5 μM and 50 ± 2 μM) (Fig. S5B).

3.4 Sympathetic nerves are not implicated in TRPM3-mediated vasodilation

The tone of mesenteric arteries is regulated by sympathetic innervation through the release of noradrenaline. The dominant effect of noradrenaline on mesenteric arteries is α_1-adrenoreceptor-mediated vasoconstriction, but mesenteric VSMC also express β_2-adrenoreceptors, whose activation could induce vasodilation. If TRPM3 channels were also expressed in sympathetic nerve endings, PS-induced dilation of mesenteric arteries could be partly mediated by the activation of β_2-adrenoreceptors. We used several approaches to assess this possibility. First, we studied the functional contribution of β_2-adrenoreceptors to the sympathetic response. The application of 20 μM noradrenaline

led to a vasoconstriction that was not affected by the application of the selective β_2-antagonist propranolol (1 µM and 5 µM). This suggests that the effects of sympathetic stimulation on mesenteric vessels are exclusively mediated by noradrenaline acting on α_1-adrenoreceptors (Fig. 6A). Consistently with this, we failed to find any vasodilation in response to noradrenaline application in Phe-pre-contracted arteries (Fig. 6B). In another series of experiments, we found that 10 µM PS-induced vasodilation was unchanged in the presence of 5 µM propranolol (Fig. 6C, 40.3 ± 1.2 µM in the presence of propranolol; 38.5 ± 0.9 µM when only PS was applied), further indicating that β_2-adrenoreceptors are not involved in the vasodilation induced by PS. In addition, we performed double immunostainings of intact mesenteric arteries of *Trpm3* KO mice using anti-β-gal and anti-Tyrosine hydroxylase (TH) antibodies. Due to their proximity, we could not distinguish the sympathetic nerves from the sensory fibers in the thick nerve bundles present in the adventitial layer (Fig. 7, adventitia, left panels), however we could find single β-gal-positive structures in the adventitia that are clearly not stained for TH (Fig. 7, white arrow heads from merged left panel). Furthermore, we also found a distinctively clear network of TH-positive sympathetic nerves closer to the medial layer, in which β-gal was not detected (Fig. 7, advent. + VSMC, right panels). Altogether, these experiments exclude an involvement of sympathetic fibers in TRPM3-mediated vasodilation.

3.5 CGRP release induces vasodilation via activation of K^+ channels

Next, we explored the mechanisms by which CGRP receptor activation in VSMC leads to vasodilation. Stimulation of the CGRP receptor has been reported to increase cyclic adenosine monophosphate (cAMP) production via the adenylate cyclase (AC) [30] and may therefore lead to protein kinase A (PKA)-mediated activation of K^+ channels in

VSMC and consequent hyperpolarization and arterial relaxation. To test whether activation of K^+ channels is involved in the vasodilation response triggered by TRPM3 activation we compared the effects of 10 µM PS in arteries treated or not with K^+ channel blockers. We noticed that the vasodilation induced by acute application of 10 µM PS (42 ± 4 %) in the presence of phenylephrine (10 µM) (Fig. 8A) was larger than that induced by the same concentration during the cumulative dose-response experiments (18 ± 4%). This may be due to partial CGRP depletion induced by previous applications of PS at low concentrations. Nevertheless, the effects of cumulative (Fig. 5D) or acute (Fig. S6) application of 10 µM PS were largely mediated by CGRP. Pretreatment with the voltage- and Ca^{2+}-activated K^+ channel blocker paxilline (500 nM) [31] and the K_V1 channels blocker correolide (10 µM) [32] led to a significant reduction of the effect of PS on pre-contracted mesenteric arteries. This effect was enhanced by addition of the K_V2 blocker stromatoxin (ScTx1, 50 nM) (Fig. 8A, B) [33]. None of these compounds affected the responses of HEK293T cells stably transfected with mouse TRPM3 to PS (Fig. S7A), indicating that they did not target TRPM3 in the arterial preparations. We also probed for direct modulatory effects of PS on K_V channels in whole-cell patch-clamp experiments performed in mesenteric VSMC freshly isolated from WT and *Trpm3* KO mice. Current-voltage relationships elicited in WT and in *Trpm3* KO VSMC by depolarizing pulses were unaffected by application of PS (10 and 30 µM; Fig. S7B, C).

We further assessed the implication of the cAMP pathway and K^+ channels by testing the effects of forskolin, a direct activator of AC, both in the absence and in the presence of paxilline, correolide and stromatoxin. We found 1 µM forskolin to induce strong vasodilation, an effect that was significantly attenuated in the presence of the K^+ channel blockers (Fig. 8C, D). Taken together, these results indicate that the TRPM3-

435 mediated dilation of mesenteric arteries is at least partly mediated by the activation of
436 K_V channels in VSMC.

437 **4. Discussion**

438 TRP channels have been found in all cell types relevant for vascular function.
439 Endothelial TRP channels regulate angiogenesis and vascular tone and permeability,
440 whereas in VSMC they are implicated in the regulation of contraction and proliferation
441 [2, 34]. TRP channels are also expressed in perivascular cells, such as TRPV4 in
442 astrocytes and TRPV1 and TRPA1 in sensory neurons [2]. Here we investigated the
443 expression and functional role of an emerging sensory TRP channel, TRPM3, in
444 resistance arteries.

445 Although we found *Trpm3* mRNA in VSMC and adventitia layer (Fig. 1A, B), our
446 anatomical and functional data are consistent with an expression of TRPM3 protein
447 restricted to perivascular nerve endings (Figs. 1C and D, 2, 3, 4, 5E, 7 and S2). A
448 previous report showed functional expression of TRPM3 channels in proliferating
449 human VSMC and in freshly isolated mouse aortic myocytes [17], but we did not find
450 responses to PS in freshly isolated mouse mesenteric myocytes (Fig. 4A, B). Whether
451 these differences may reflect vascular bed-dependent functional expression of TRPM3
452 requires further investigation. Our qPCR studies show that *Trpm3* mRNA expression is
453 almost 40 times higher in aorta than in mesenteric arteries (data not shown). This is in
454 line with TRPM3 channels being functionally expressed in aortic VSMC, activation of
455 which leads to Ca^{2+} entry and vasoconstriction [17].

456 In contrast to these previous observations in aorta [17], we found that PS induces
457 vasodilation of mesenteric arteries (Fig. 5A). The maximal effect of this compound was

458 comparable to the maximal dilation induced by nifedipine or a Ca^{2+} free solution (Fig.
459 S1). A previous report showed that genetic ablation of *Trpm3* abolished CGRP release
460 from skin and insulin secretion from isolated pancreatic islets in response to 100 μM PS
461 [18]. However, we found that PS induced dilation via two components, being the high
462 EC_{50} component still present in arteries isolated from *Trpm3* KO mice (Fig. 5B, D). Our
463 results show that PS has TRPM3-independent effects in mesenteric arteries at
464 concentrations higher than 10 μM. This compound has been shown to act on other
465 targets, such as the gamma-aminobutyric acid receptor A and the N-methyl-D-aspartate
466 receptor [35], but it is not yet clear whether these bare any relevance in mesenteric
467 arteries. Of note, the values of the EC_{50} and Hill coefficient corresponding to the
468 TRPM3-independent PS responses were different in WT and *Trpm3* KO arteries. This
469 may be due to the fact that in WT arteries the TRPM3-dependent processes may affect
470 the TRPM3-independent vasodilation observed at higher PS concentrations. The
471 nonlinear and integrative character of the vasodilation process may preclude that the
472 effects of individual PS-dependent components add up in a simple arithmetic way.
473 Further assessment of this observation will be possible once the mechanism underlying
474 the latter component is clarified. Nevertheless, the data fitting results indicate that the
475 TRPM3-dependent component contributes to an important fraction of the total PS-
476 induced dilation of WT arteries (~60%), and its occurrence in the lower concentration
477 range suggest that it is the most relevant component in physiological conditions.

478 In regard to the mechanism underlying TRPM3-dependent vasodilation, the overlap we
479 observed between the PS dose response curves obtained for *Trpm3* KO arteries and for
480 WT arteries in the presence of the CGRP receptor inhibitor suggests that PS-induced
481 CGRP effects are fully mediated by TRPM3 (Fig. 5D). Previous studies demonstrated
482 CGRP release upon TRP channel activation in mouse trachea [36] and hind paw skin

[18]. However, we were unable to detect CGRP release from mesenteric using similar experimental procedures (data not shown), most likely because our preparation is between ~200 and 2000-fold smaller than the trachea and skin ones, respectively.

The mechanisms proposed for the vasodilating effects of CGRP include an endothelium-dependent component, whereby activation of the endothelial CGRP receptor results in a rise in cAMP, NO production and guanylate cyclase-mediated vasodilation [37]. In addition, there are two effects mediated by AC and PKA stimulation in VSMC: activation of K^+ channels and stimulation of myosin light chain phosphatase [28, 38]. Our data are consistent with all these mechanisms, as we found that the responses to PS were enhanced in the presence of endothelium and were partially inhibited by a cocktail of K^+ channel blockers (Fig. S5 and 8A, respectively). Furthermore, we could exclude a possible contribution of sympathetic fibers to the PS-induced vasodilation mechanisms. Our data exclude both the functional contribution of β_2-adrenoreceptors to the sympathetic response and the involvement of these receptors in the vasodilation induced by PS application, as no differences were observed when we applied the β-blocker propranolol (Fig. 6). Moreover, the absence of colocalization of TH and β-gal in the nerve fibers innervating the media layer of the mesenteric arteries is also consistent with the lack of expression of TRPM3 in sympathetic nerve endings.

Notably, the vasodilation we report here is the most sensitive TRPM3-mediated tissue response to PS reported so far. Previous studies showed TRPM3-dependent effects of PS in the range of tens to hundreds of micromolar, e.g., insulin release from pancreatic islets [21], CGRP release form mouse skin preparations [18] and rat ductus arteriousus contraction [39]. In contrast, we found significant TRPM3-dependent vasodilation with an EC_{50} of 7.7 μM in intact arteries. This value is the most similar to those reported for

stimulation of TRPM3 currents *in vitro* (5 - 23 μM) [40, 41]. Most likely, this is a consequence of the technical approach in myography experiments since PS has direct access to the TRPM3-expressing nerve endings, which contrasts with other preparations in which structural barriers are expected to interfere with PS diffusion. This suggests the mesenteric artery preparation as very instrumental for studies on TRPM3 modulation and pharmacology, including the testing of the specificity of previously described channel inhibitors [42, 43], in a close-to-physiological context. In addition, our results shed light on the long-standing question of whether PS is after all a physiological endogenous agonist of TRPM3 [21]. We observed TRPM3-dependent vasodilation induced by PS in the low micromolar range (Fig. 5A), which matches PS concentrations that may be present in living tissues [21]. The physiological or pathological contexts in which PS reaches such concentrations in mesenteric tissue remain, however, elusive. The idea that TRPM3 activation induces vasodilation in mesenteric arteries is further supported by the potent effect of the synthetic agonist CIM0216. However, this compound proved not to be fully specific for this channel, as it also produced vasodilation in arteries dissected from *Trpm3* KO mice at concentrations above ~0.1 μM (Fig. S4). We argue, therefore, that CIM0216 may be used as pharmacological tool to further investigate the role of TRPM3 in mesenteric arteries below these concentrations. Because this is a synthetic compound with no obvious similarity to any other known TRPM3 modulator [18], we consider that investigating the TRPM3-independent effects is interesting but beyond the scope of the present study. Nevertheless, reporting for the first time that CIM0216 has off-target effects is of great value for future research on TRPM3 pathophysiology.

The functional expression of TRPM3 in nociceptive neurons and its contribution to noxious heat sensing [19] may suggest that the function of this channel in mesenteric

arteries is the detection of noxious stimuli generated in pathological conditions. The high temperatures required for TRPM3 activation [19] strongly indicate that heat may not be a relevant stimulus of TRPM3 in mesenteric preparations. Nevertheless, it would be interesting to determine whether this channel is implicated in responses of skin resistance arteries to heat. However, in contrast to previous reports in skin and trachea [18, 19], we show here for the first time a role of TRPM3 in sensory fibers innervating a tissue that is not directly accessible to external stimuli. This may indicate that TRPM3 functions as detector of endogenous compounds released upon tissue damage and/or metabolic deregulation. Two other sensory TRP channels, TRPV1 and TRPA1 are proposed to act as receptors of danger- and pathogen-associated molecular patterns during tissue injury and inflammatory diseases [44], by detecting acidosis, reactive oxygen and nitrogen species, electrophilic compounds and bacterial endotoxins [2, 8, 36, 45-48]. However, TRPV1 and TRPA1 have also been reported in VSMC and endothelial cells of resistance arteries, respectively [49-53]. Thus, according to our findings, TRPM3 is the only one of these sensory TRP channels exclusively functional in perivascular nerves. This suggests TRPM3 as the most specific target to trigger resistance artery vasodilation via stimulation of the perivascular sensory innervation.

We conclude that in contrast to what was previously reported in aorta [17], in mesenteric arteries TRPM3 is functionally expressed mainly in perivascular nerve endings and its activation leads to vasodilation rather than contraction. Our data is consistent with a model in which activation of TRPM3 triggers CGRP release, leading to vasodilation via endothelium-dependent and endothelium-independent pathways. We propose that, together with TRPV1 and TRPA1, TRPM3 allows mesenteric arteries to react to a wide range of damage-associated molecules, leading to vasodilation, via the common pathway of CGRP release from perivascular sensory nerve endings.

Funding

This work was supported by grants from the Fund for Scientific Research Flanders (G.0C68.15), the Ministerio de Economía y Competitividad (MINECO), BFU2013-45867-R and BFU2016-75360-R to JRLL and MTPG and Junta de Castilla y León Grant VA114P17 to MTPG. Y.A.A. is a Postdoctoral Fellow of the FWO.

Acknowledgments

We thank the members of the Laboratory of Ion Channel Research for helpful discussions and specially Prof. J. Vriens for providing the TRPM3 agonist CIM0216. We also thank T. Arranz and E. Alonso for excellent technical assistance.

Disclosures

None.

References

[1] L. Alonso-Carbajo, M. Kecskes, G. Jacobs, A. Pironet, N. Syam, K. Talavera, R. Vennekens, Muscling in on TRP channels in vascular smooth muscle cells and cardiomyocytes, Cell Calcium 66 (2017) 48-61.
[2] S. Earley, J.E. Brayden, Transient receptor potential channels in the vasculature, Physiol Rev 95(2) (2015) 645-90.
[3] G. Owsianik, K. Talavera, T. Voets, B. Nilius, Permeation and selectivity of TRP channels, Annu Rev Physiol 68 (2006) 685-717.
[4] I. Alvarez-Miguel, P. Cidad, M.T. Perez-Garcia, J.R. Lopez-Lopez, Differences in TRPC3 and TRPC6 channels assembly in mesenteric vascular smooth muscle cells in essential hypertension, J Physiol 595(5) (2017) 1497-1513.
[5] M. Mederos y Schnitzler, U. Storch, S. Meibers, P. Nurwakagari, A. Breit, K. Essin, M. Gollasch, T. Gudermann, Gq-coupled receptors as mechanosensors mediating myogenic vasoconstriction, EMBO J 27(23) (2008) 3092-103.
[6] S. Earley, T.J. Heppner, M.T. Nelson, J.E. Brayden, TRPV4 forms a novel Ca2+ signaling complex with ryanodine receptors and BKCa channels, Circ Res 97(12) (2005) 1270-9.
[7] S. Earley, T. Pauyo, R. Drapp, M.J. Tavares, W. Liedtke, J.E. Brayden, TRPV4-dependent dilation of peripheral resistance arteries influences arterial pressure, Am J Physiol Heart Circ Physiol 297(3) (2009) H1096-102.
[8] D.M. Bautista, P. Movahed, A. Hinman, H.E. Axelsson, O. Sterner, E.D. Hogestatt, D. Julius, S.E. Jordt, P.M. Zygmunt, Pungent products from garlic activate the sensory ion channel TRPA1, Proc Natl Acad Sci U S A 102(34) (2005) 12248-52.

590 [9] L.H. Wang, M. Luo, Y. Wang, J.J. Galligan, D.H. Wang, Impaired vasodilation in response
591 to perivascular nerve stimulation in mesenteric arteries of TRPV1-null mutant mice, J
592 Hypertens 24(12) (2006) 2399-408.
593 [10] Y. Li, R.L. Baylie, M.J. Tavares, J.E. Brayden, TRPM4 channels couple purinergic
594 receptor mechanoactivation and myogenic tone development in cerebral parenchymal arterioles,
595 J Cereb Blood Flow Metab 34(10) (2014) 1706-14.
596 [11] C.J. Garland, S.V. Smirnov, P. Bagher, C.S. Lim, C.Y. Huang, R. Mitchell, C. Stanley, A.
597 Pinkney, K.A. Dora, TRPM4 inhibitor 9-phenanthrol activates endothelial cell intermediate
598 conductance calcium-activated potassium channels in rat isolated mesenteric artery, Br J
599 Pharmacol 172(4) (2015) 1114-23.
600 [12] C.M. Hecquet, G.U. Ahmmed, S.M. Vogel, A.B. Malik, Role of TRPM2 channel in
601 mediating H2O2-induced Ca2+ entry and endothelial hyperpermeability, Circ Res 102(3)
602 (2008) 347-55.
603 [13] A. Zholos, Pharmacology of transient receptor potential melastatin channels in the
604 vasculature, Br J Pharmacol 159(8) (2010) 1559-71.
605 [14] C. Grimm, R. Kraft, S. Sauerbruch, G. Schultz, C. Harteneck, Molecular and functional
606 characterization of the melastatin-related cation channel TRPM3, J Biol Chem 278(24) (2003)
607 21493-501.
608 [15] N. Lee, J. Chen, L. Sun, S. Wu, K.R. Gray, A. Rich, M. Huang, J.H. Lin, J.N. Feder, E.B.
609 Janovitz, P.C. Levesque, M.A. Blanar, Expression and characterization of human transient
610 receptor potential melastatin 3 (hTRPM3), J Biol Chem 278(23) (2003) 20890-7.
611 [16] J. Oberwinkler, S.E. Philipp, TRPM3, Handb Exp Pharmacol 222 (2014) 427-59.
612 [17] J. Naylor, J. Li, C.J. Milligan, F. Zeng, P. Sukumar, B. Hou, A. Sedo, N. Yuldasheva, Y.
613 Majeed, D. Beri, S. Jiang, V.A. Seymour, L. McKeown, B. Kumar, C. Harteneck, D. O'Regan,
614 S.B. Wheatcroft, M.T. Kearney, C. Jones, K.E. Porter, D.J. Beech, Pregnenolone sulphate- and
615 cholesterol-regulated TRPM3 channels coupled to vascular smooth muscle secretion and
616 contraction, Circ Res 106(9) (2010) 1507-15.
617 [18] K. Held, T. Kichko, K. De Clercq, H. Klaassen, R. Van Bree, J.C. Vanherck, A. Marchand,
618 P.W. Reeh, P. Chaltin, T. Voets, J. Vriens, Activation of TRPM3 by a potent synthetic ligand
619 reveals a role in peptide release, Proc Natl Acad Sci U S A 112(11) (2015) E1363-72.
620 [19] J. Vriens, G. Owsianik, T. Hofmann, S.E. Philipp, J. Stab, X. Chen, M. Benoit, F. Xue, A.
621 Janssens, S. Kerselaers, J. Oberwinkler, R. Vennekens, T. Gudermann, B. Nilius, T. Voets,
622 TRPM3 is a nociceptor channel involved in the detection of noxious heat, Neuron 70(3) (2011)
623 482-94.
624 [20] S. Hughes, C.A. Pothecary, A. Jagannath, R.G. Foster, M.W. Hankins, S.N. Peirson,
625 Profound defects in pupillary responses to light in TRPM-channel null mice: a role for TRPM
626 channels in non-image-forming photoreception, Eur J Neurosci 35(1) (2012) 34-43.
627 [21] T.F. Wagner, S. Loch, S. Lambert, I. Straub, S. Mannebach, I. Mathar, M. Dufer, A. Lis,
628 V. Flockerzi, S.E. Philipp, J. Oberwinkler, Transient receptor potential M3 channels are
629 ionotropic steroid receptors in pancreatic beta cells, Nat Cell Biol 10(12) (2008) 1421-30.
630 [22] H.C. Chen, J. Xie, Z. Zhang, L.T. Su, L. Yue, L.W. Runnels, Blockade of TRPM7 channel
631 activity and cell death by inhibitors of 5-lipoxygenase, PLoS One 5(6) (2010) e11161.
632 [23] R.A. Nicholas, W.C. Watt, E.R. Lazarowski, Q. Li, K. Harden, Uridine nucleotide
633 selectivity of three phospholipase C-activating P2 receptors: identification of a UDP-selective, a
634 UTP-selective, and an ATP- and UTP-specific receptor, Mol Pharmacol 50(2) (1996) 224-9.
635 [24] C.A. Maggi, Tachykinins and calcitonin gene-related peptide (CGRP) as co-transmitters
636 released from peripheral endings of sensory nerves, Prog Neurobiol 45(1) (1995) 1-98.
637 [25] D. van Rossum, U.K. Hanisch, R. Quirion, Neuroanatomical localization, pharmacological
638 characterization and functions of CGRP, related peptides and their receptors, Neurosci
639 Biobehav Rev 21(5) (1997) 649-78.
640 [26] A. Fujimori, A. Saito, S. Kimura, T. Watanabe, Y. Uchiyama, H. Kawasaki, K. Goto,
641 Neurogenic vasodilation and release of calcitonin gene-related peptide (CGRP) from
642 perivascular nerves in the rat mesenteric artery, Biochem Biophys Res Commun 165(3) (1989)
643 1391-8.

[27] R. Uddman, T. Grunditz, F. Sundler, Calcitonin gene related peptide: a sensory transmitter in dental pulps?, Scand J Dent Res 94(3) (1986) 219-24.
[28] S.D. Brain, A.D. Grant, Vascular actions of calcitonin gene-related peptide and adrenomedullin, Physiol Rev 84(3) (2004) 903-34.
[29] F.A. Russell, R. King, S.J. Smillie, X. Kodji, S.D. Brain, Calcitonin gene-related peptide: physiology and pathophysiology, Physiol Rev 94(4) (2014) 1099-142.
[30] F. Van Valen, G. Piechot, H. Jurgens, Calcitonin gene-related peptide (CGRP) receptors are linked to cyclic adenosine monophosphate production in SK-N-MC human neuroblastoma cells, Neurosci Lett 119(2) (1990) 195-8.
[31] H.G. Knaus, O.B. McManus, S.H. Lee, W.A. Schmalhofer, M. Garcia-Calvo, L.M. Helms, M. Sanchez, K. Giangiacomo, J.P. Reuben, A.B. Smith, 3rd, et al., Tremorgenic indole alkaloids potently inhibit smooth muscle high-conductance calcium-activated potassium channels, Biochemistry 33(19) (1994) 5819-28.
[32] J.P. Felix, R.M. Bugianesi, W.A. Schmalhofer, R. Borris, M.A. Goetz, O.D. Hensens, J.M. Bao, F. Kayser, W.H. Parsons, K. Rupprecht, M.L. Garcia, G.J. Kaczorowski, R.S. Slaughter, Identification and biochemical characterization of a novel nortriterpene inhibitor of the human lymphocyte voltage-gated potassium channel, Kv1.3, Biochemistry 38(16) (1999) 4922-30.
[33] P. Escoubas, S. Diochot, M.L. Celerier, T. Nakajima, M. Lazdunski, Novel tarantula toxins for subtypes of voltage-dependent potassium channels in the Kv2 and Kv4 subfamilies, Mol Pharmacol 62(1) (2002) 48-57.
[34] Z. Yue, J. Xie, A.S. Yu, J. Stock, J. Du, L. Yue, Role of TRP channels in the cardiovascular system, Am J Physiol Heart Circ Physiol 308(3) (2015) H157-82.
[35] C. Harteneck, Pregnenolone sulfate: from steroid metabolite to TRP channel ligand, Molecules 18(10) (2013) 12012-28.
[36] V. Meseguer, Y.A. Alpizar, E. Luis, S. Tajada, B. Denlinger, O. Fajardo, J.A. Manenschijn, C. Fernandez-Pena, A. Talavera, T. Kichko, B. Navia, A. Sanchez, R. Senaris, P. Reeh, M.T. Perez-Garcia, J.R. Lopez-Lopez, T. Voets, C. Belmonte, K. Talavera, F. Viana, TRPA1 channels mediate acute neurogenic inflammation and pain produced by bacterial endotoxins, Nat Commun 5 (2014) 3125.
[37] D.W. Gray, I. Marshall, Human alpha-calcitonin gene-related peptide stimulates adenylate cyclase and guanylate cyclase and relaxes rat thoracic aorta by releasing nitric oxide, Br J Pharmacol 107(3) (1992) 691-6.
[38] X. Yu, F. Li, E. Klussmann, J.N. Stallone, G. Han, G protein-coupled estrogen receptor 1 mediates relaxation of coronary arteries via cAMP/PKA-dependent activation of MLCP, Am J Physiol Endocrinol Metab 307(4) (2014) E398-407.
[39] R. Aoki, U. Yokoyama, Y. Ichikawa, M. Taguri, S. Kumagaya, R. Ishiwata, C. Yanai, S. Fujita, M. Umemura, T. Fujita, S. Okumura, M. Sato, S. Minamisawa, T. Asou, M. Masuda, S. Iwasaki, S. Nishimaki, K. Seki, S. Yokota, Y. Ishikawa, Decreased serum osmolality promotes ductus arteriosus constriction, Cardiovasc Res 104(2) (2014) 326-36.
[40] A. Drews, F. Mohr, O. Rizun, T.F. Wagner, S. Dembla, S. Rudolph, S. Lambert, M. Konrad, S.E. Philipp, M. Behrendt, S. Marchais-Oberwinkler, D.F. Covey, J. Oberwinkler, Structural requirements of steroidal agonists of transient receptor potential melastatin 3 (TRPM3) cation channels, Br J Pharmacol 171(4) (2014) 1019-32.
[41] J. Oberwinkler, A. Lis, K.M. Giehl, V. Flockerzi, S.E. Philipp, Alternative splicing switches the divalent cation selectivity of TRPM3 channels, J Biol Chem 280(23) (2005) 22540-8.
[42] U. Krugel, I. Straub, H. Beckmann, M. Schaefer, Primidone inhibits TRPM3 and attenuates thermal nociception in vivo, Pain 158(5) (2017) 856-867.
[43] I. Straub, U. Krugel, F. Mohr, J. Teichert, O. Rizun, M. Konrad, J. Oberwinkler, M. Schaefer, Flavanones that selectively inhibit TRPM3 attenuate thermal nociception in vivo, Mol Pharmacol 84(5) (2013) 736-50.
[44] G. Santoni, C. Cardinali, M.B. Morelli, M. Santoni, M. Nabissi, C. Amantini, Danger- and pathogen-associated molecular patterns recognition by pattern-recognition receptors and ion channels of the transient receptor potential family triggers the inflammasome activation in immune cells and sensory neurons, J Neuroinflammation 12 (2015) 21.

[45] B. Boonen, Y.A. Alpizar, V.M. Meseguer, K. Talavera, TRP Channels as Sensors of Bacterial Endotoxins, Toxins (Basel) 10(8) (2018).
[46] B. Boonen, Y.A. Alpizar, A. Sanchez, A. Lopez-Requena, T. Voets, K. Talavera, Differential effects of lipopolysaccharide on mouse sensory TRP channels, Cell Calcium 73 (2018) 72-81.
[47] M. Eberhardt, M. Dux, B. Namer, J. Miljkovic, N. Cordasic, C. Will, T.I. Kichko, J. de la Roche, M. Fischer, S.A. Suarez, D. Bikiel, K. Dorsch, A. Leffler, A. Babes, A. Lampert, J.K. Lennerz, J. Jacobi, M.A. Marti, F. Doctorovich, E.D. Hogestatt, P.M. Zygmunt, I. Ivanovic-Burmazovic, K. Messlinger, P. Reeh, M.R. Filipovic, H2S and NO cooperatively regulate vascular tone by activating a neuroendocrine HNO-TRPA1-CGRP signalling pathway, Nat Commun 5 (2014) 4381.
[48] M.N. Sullivan, A.L. Gonzales, P.W. Pires, A. Bruhl, M.D. Leo, W. Li, A. Oulidi, F.A. Boop, Y. Feng, J.H. Jaggar, D.G. Welsh, S. Earley, Localized TRPA1 channel Ca2+ signals stimulated by reactive oxygen species promote cerebral artery dilation, Sci Signal 8(358) (2015) ra2.
[49] D.J. Cavanaugh, A.T. Chesler, A.C. Jackson, Y.M. Sigal, H. Yamanaka, R. Grant, D. O'Donnell, R.A. Nicoll, N.M. Shah, D. Julius, A.I. Basbaum, Trpv1 reporter mice reveal highly restricted brain distribution and functional expression in arteriolar smooth muscle cells, J Neurosci 31(13) (2011) 5067-77.
[50] A. Czikora, I. Rutkai, E.T. Pasztor, A. Szalai, R. Porszasz, J. Boczan, I. Edes, Z. Papp, A. Toth, Different desensitization patterns for sensory and vascular TRPV1 populations in the rat: expression, localization and functional consequences, PLoS One 8(11) (2013) e78184.
[51] S. Earley, A.L. Gonzales, R. Crnich, Endothelium-dependent cerebral artery dilation mediated by TRPA1 and Ca2+-Activated K+ channels, Circ Res 104(8) (2009) 987-94.
[52] T. Kark, Z. Bagi, E. Lizanecz, E.T. Pasztor, N. Erdei, A. Czikora, Z. Papp, I. Edes, R. Porszasz, A. Toth, Tissue-specific regulation of microvascular diameter: opposite functional roles of neuronal and smooth muscle located vanilloid receptor-1, Mol Pharmacol 73(5) (2008) 1405-12.
[53] X. Qian, M. Francis, V. Solodushko, S. Earley, M.S. Taylor, Recruitment of dynamic endothelial Ca2+ signals by the TRPA1 channel activator AITC in rat cerebral arteries, Microcirculation 20(2) (2013) 138-48.

731 **Figure legends**

732 **Figure 1.** TRPM3 is located in perivascular nerve endings of mouse mesenteric arteries.
733 (*A*) Relative expression of *Trpm* genes in mesenteric arteries dissected from WT mice.
734 Data are represented as mean ± SEM, $*P < 0.05$; $^{\#}P < 0.01$ (n = 3), one way ANOVA,
735 Dunn-Sidak test. (*B*) Relative expression of *Trpm* genes in endothelium-denuded
736 arteries using arteries with endothelium as calibrator. Data are mean ± SEM of
737 triplicates (n = 3 different pools of arteries from 5 different mice). (*C*) Confocal images
738 of intact WT mouse mesenteric arteries labeled with PGP9.5 (left) and TRPM3 (center)
739 antibodies. An overlay of these images merged with a nuclear staining DAPI (blue) is
740 shown on the right. (*D*) Confocal microscopy images of the adventitia and medial layers
741 labeled with a TRPM3 antibody (green) and nuclear DAPI staining (blue). The white
742 arrowheads in the bottom-right image point to TRPM3 labeling observed only in the
743 adventitial layer. Images are representative of at least 3 independent experiments.

744 **Figure 2.** Location of the transgene product of the *Trpm3* KO mice in perivascular
745 nerve endings of mesenteric arteries. (*A*) *Z*-stack confocal images of intact *Trpm3* KO
746 mouse mesenteric arteries at the levels of the adventitial (a), medial (b) and endothelial
747 (c) layers, labeled with β-galactosidase (green), PGP9.5 (red) antibodies and nuclear
748 DAPI (blue) staining. The images are representative of at least 3 independent
749 experiments. (*B*) Confocal microscopy images of the adventitial layer of a WT mouse
750 mesenteric artery labeled with β-galactosidase (green), PGP9.5 (red) antibodies and
751 nuclear DAPI staining (blue). Images are representative of at least 3 independent
752 experiments.

753 **Figure 3.** The transgene product of the *Trpm3* KO mice is not located in smooth muscle
754 layer from mesenteric arteries. Confocal microscopy images of the medial layer (*A*) and

adventital layer (*B*) of *Trpm3* KO mouse intact mesenteric arteries labeled with β-galactosidase (green), α-smooth muscle actin (red) antibodies and nuclear DAPI staining (blue). Images are representative of at least 3 independent experiments.

Figure 4. TRPM3 is not functionally expressed in WT mouse mesenteric VSMC. (*A*) Left, time course of the amplitude of currents recorded at -80 and +80 mV in control and in the presence of 10 and 30 μM PS. Right, average of current traces recorded in control (black) and in the presence of 30 μM PS (grey). (*B, C*) Left, representative examples of the time course of the amplitude of currents recorded at -150 and +80 mV, showing the effects of 100 μM UTP, 10 μM PS and 2 μM CIM0216. Right, the traces represent the differences between traces recorded in the presence of these compounds at the time points indicated by the labels a and b and a corresponding current trace recorded in control.

Figure 5. TRPM3-induced vasodilation of mesenteric arteries is mediated by CGRP receptor activation. Representative examples of the effects of increasing concentrations of pregnenolone sulfate (PS, in μM) on the diameter of arteries dissected from WT (*A*) and *Trpm3* KO mice (*B*) in the presence of phenylephrine (Phe, 10 μM). (*C*) Effects of PS (in μM) on WT arteries in the presence of the CGRP receptor antagonist BIBN 4096 (1 μM) and phenylephrine (10 μM). Nifedipine (Nif, 10 μM) was applied at the end of each experiment. (*D*) Dose dependency of PS-induced vasodilation (in μM) in precontracted arteries dissected from WT, *Trpm3* KO mice and in WT arteries in the presence of 1 μM BIBN 4096. Data are mean ± SEM (n = 10 arteries from 8 WT mice; n = 8 arteries from 7 *Trpm3* KO mice and n = 8 arteries from 6 WT animals + BIBN 4096). The black solid line represents the fit of the WT data with a two-component Hill equation. The grey solid line and the dotted line represent the fit of the data for *Trpm3*

779 KO and WT in the presence of BIBN 4096 with single-component Hill equations. *
780 indicates $P < 0.05$ compared to WT mice, unpaired t-test. (*E*) Confocal images of intact
781 *Trpm3* KO mouse mesenteric arteries of the adventitial layer labeled with β-
782 galactosidase (green), CGRP (red) antibodies and nuclear DAPI staining (blue). Images
783 are representative of at least 3 independent experiments.

784 **Figure 6.** Sympathetic perivascular nerves are not involved in TRPM3-induced
785 vasodilation of mesenteric arteries. *(A)* Representative example of the effect of
786 noradrenaline (NA, 20 μM) on a WT mouse mesentery artery in the presence of the β-
787 adrenoreceptor blocker propranolol (PRO, 1 μM in the left panel and 5 μM in the right
788 panel). *(B)* Effect of 10 μM noradrenaline on WT arteries precontracted with
789 phenylephrine (Phe, 20 μM). *(C)* Effect of pregnenolone sulfate (PS, 10 μM) in the
790 presence of propranolol (5 μM). Nifedipine (Nif, 10 μM) was applied at the end of each
791 experiment.

792 **Figure 7.** *C*onfocal images of intact *Trpm3* KO mouse mesenteric arteries at the level of
793 the adventitial (left panels) and closer to the medial (right panels) layers, labeled with
794 nuclear DAPI staining (blue), β-galactosidase (green) and Tyrosine hydroxylase (red).
795 Images are representative of at least 3 independent experiments.

796 **Figure 8.** TRPM3-dependent vasodilation is partly mediated by activation of K^+
797 channels and further stimulation of adenylate cyclase. (*A***)** Comparison of the effects of
798 pregnenolone sulfate (PS, 10 μM) in control conditions and in the presence of the K^+
799 channel blockers paxilline (500 nM), correolide (10 μM) and stromatoxin (50 nM). The
800 scheme shows the CGRP signaling cascade leading to activation of K^+ channels via
801 stimulation of adenylate cyclase (AC) and protein kinase A (PKA) in VSMC. (*B*)
802 Average vasodilator effects of 10 μM PS on WT mesenteric arteries in control

803 conditions (n = 14 arteries from 10 mice), in the presence of paxilline and correolide (n
804 = 8 arteries from 5 mice) and in the presence of paxilline, correolide and stromatoxin (n
805 = 5 arteries from 4 mice). * indicate $P < 0.05$ for the comparison with the data obtained
806 in control, unpaired t-test. (*C*) Representative example of the effect of 1 µM forskolin
807 on a WT mouse mesentery artery in control and in the presence of the K^+ channel
808 blockers paxilline (500 nM), correolide (10 µM) and stromatoxin (50 nM). (*D*) Average
809 vasodilator effect of 1 µM forskolin in the absence (n = 4 arteries from 4 mice) and in
810 the presence of K^+ channel blockers (n = 4 arteries from 4 mice). Phe = Phenylephrine;
811 Nif = nifedipine * indicates $P < 0.05$ versus control, paired t-test.

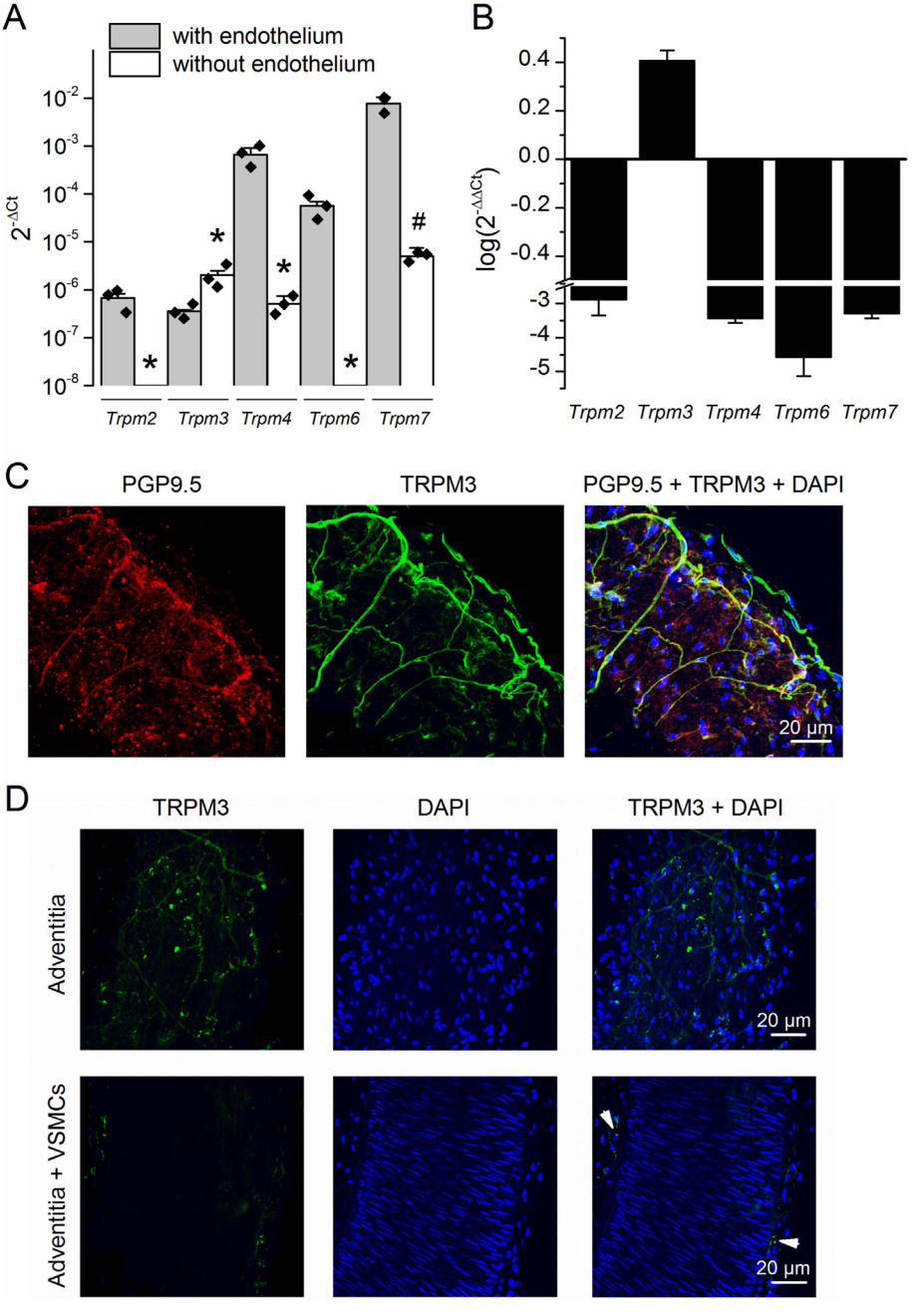
A
with endothelium
without endothelium
$2^{-\Delta Ct}$
10^{-2}
10^{-3}
10^{-4}
10^{-5}
10^{-6}
10^{-7}
10^{-8}
*
*
*
*
#
Trpm2
Trpm3
Trpm4
Trpm6
Trpm7
B
$\log(2^{-\Delta\Delta Ct})$
0.4
0.2
0.0
-0.2
-0.4
-3
-4
-5
Trpm2
Trpm3
Trpm4
Trpm6
Trpm7
C
PGP9.5
TRPM3
PGP9.5 + TRPM3 + DAPI
20 µm
D
TRPM3
DAPI
TRPM3 + DAPI
Adventitia
20 µm
Adventitia + VSMCs
20 µm

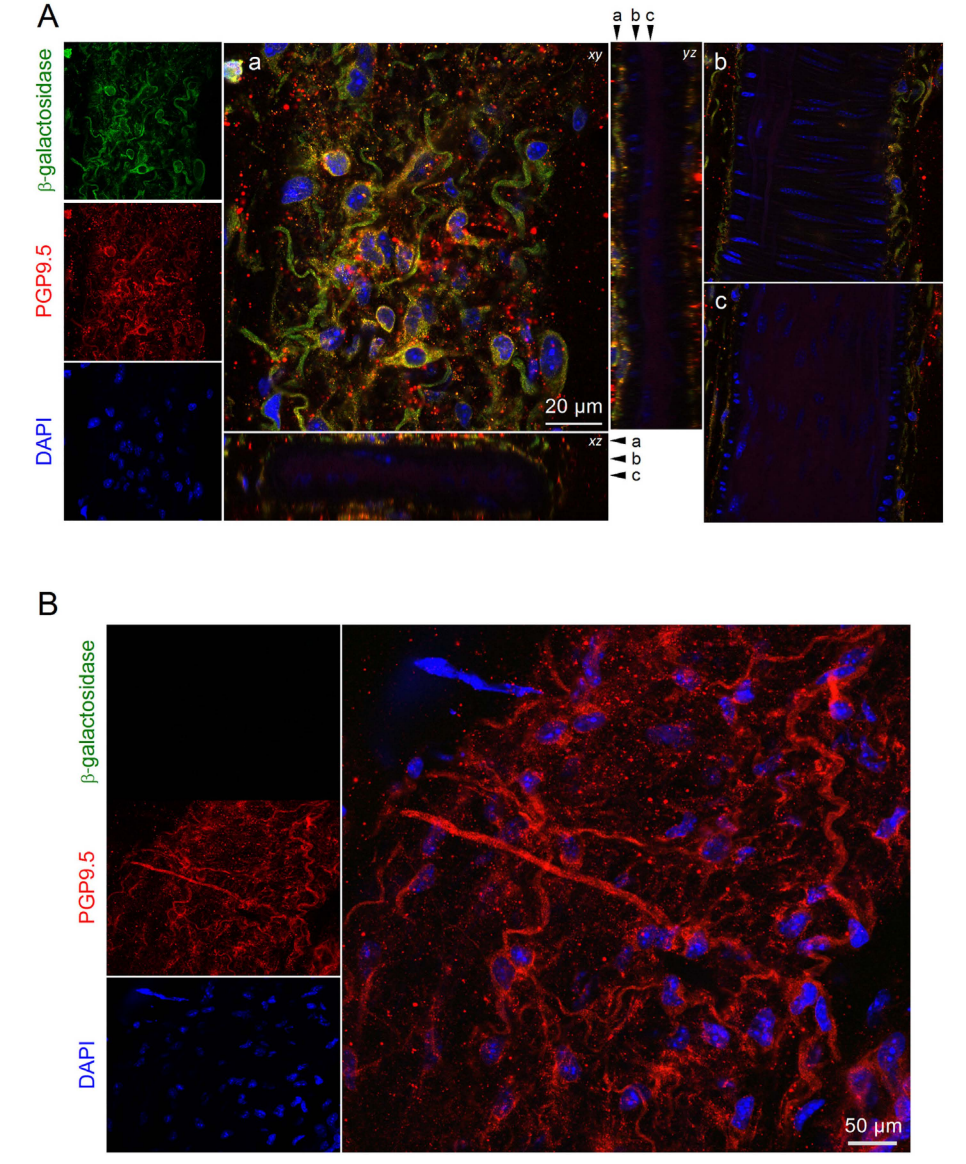
A
β-galactosidase
PGP9.5
DAPI
a
xy
yz
xz
a b c
b
c
20 μm
B
β-galactosidase
PGP9.5
DAPI
50 μm

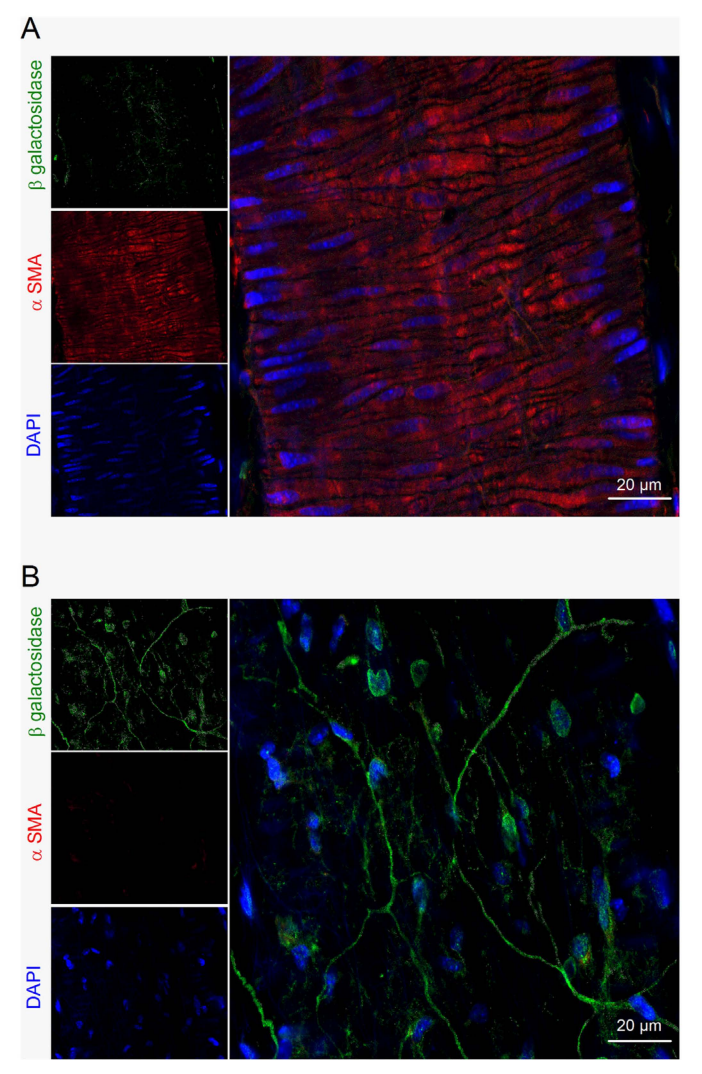
A
β galactosidase
α SMA
DAPI
20 μm
B
β galactosidase
α SMA
DAPI
20 μm

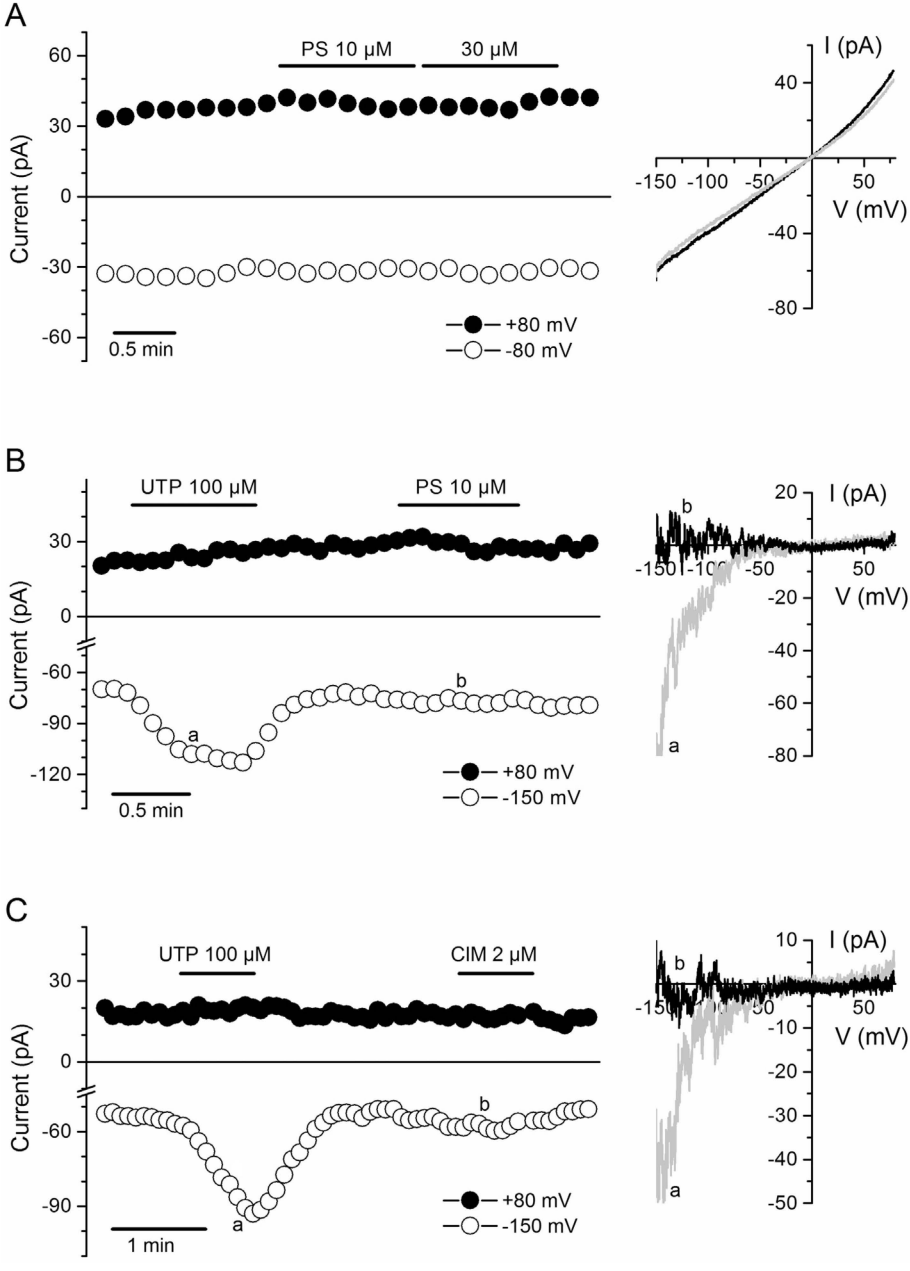
A
PS 10 μM
30 μM
Current (pA)
60
30
0
-30
-60
0.5 min
+80 mV
-80 mV
I (pA)
40
-40
-80
-150
-100
-50
50
V (mV)
B
UTP 100 μM
PS 10 μM
30
0
-60
-90
-120
a
b
0.5 min
+80 mV
-150 mV
20
-20
-40
-60
-80
C
UTP 100 μM
CIM 2 μM
1 min
10
-10
-20
-30
-40
-50

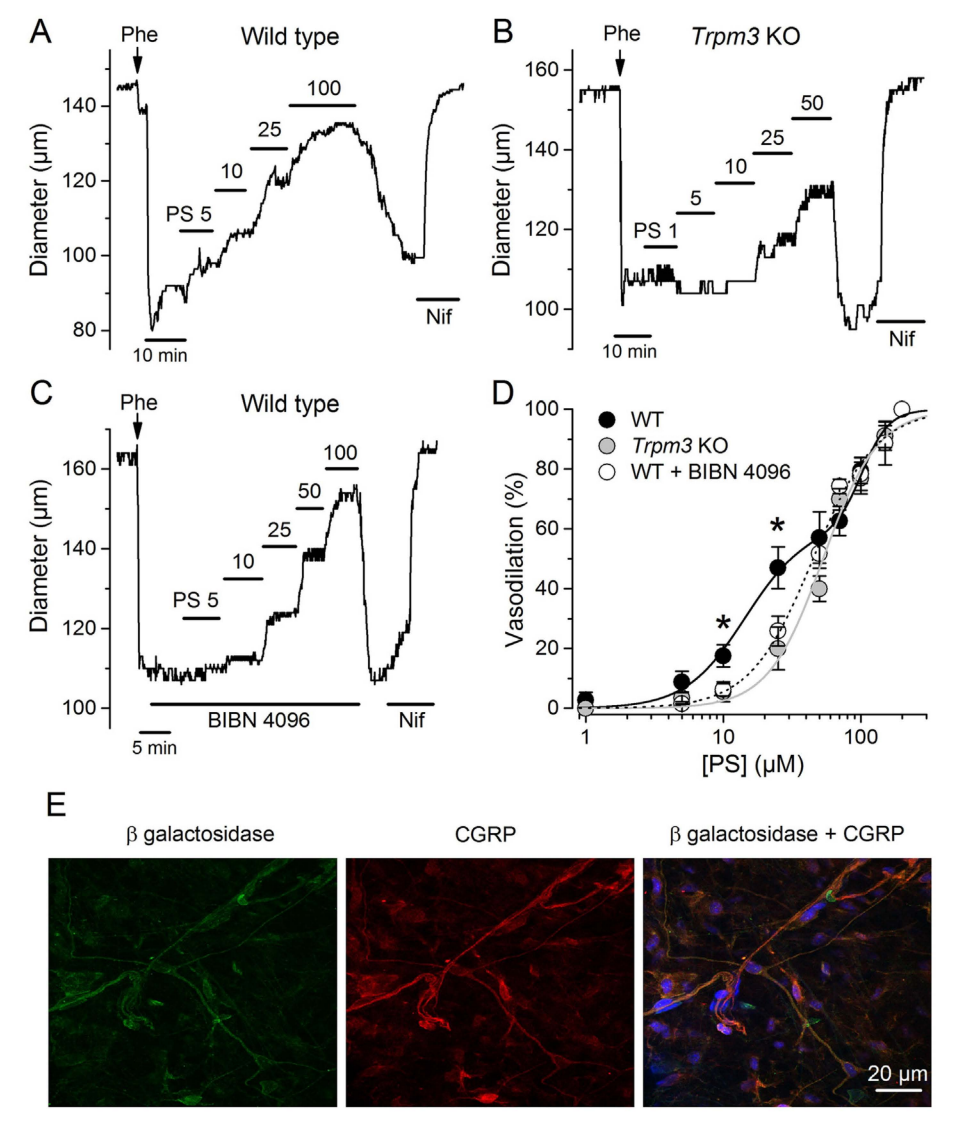
A
Phe
Wild type
Diameter (μm)
PS 5
10
25
100
10 min
Nif
B
Phe
Trpm3 KO
Diameter (μm)
PS 1
5
10
25
50
10 min
Nif
C
Phe
Wild type
Diameter (μm)
PS 5
10
25
50
100
BIBN 4096
5 min
Nif
D
WT
Trpm3 KO
WT + BIBN 4096
Vasodilation (%)
[PS] (μM)
E
β galactosidase
CGRP
β galactosidase + CGRP
20 μm

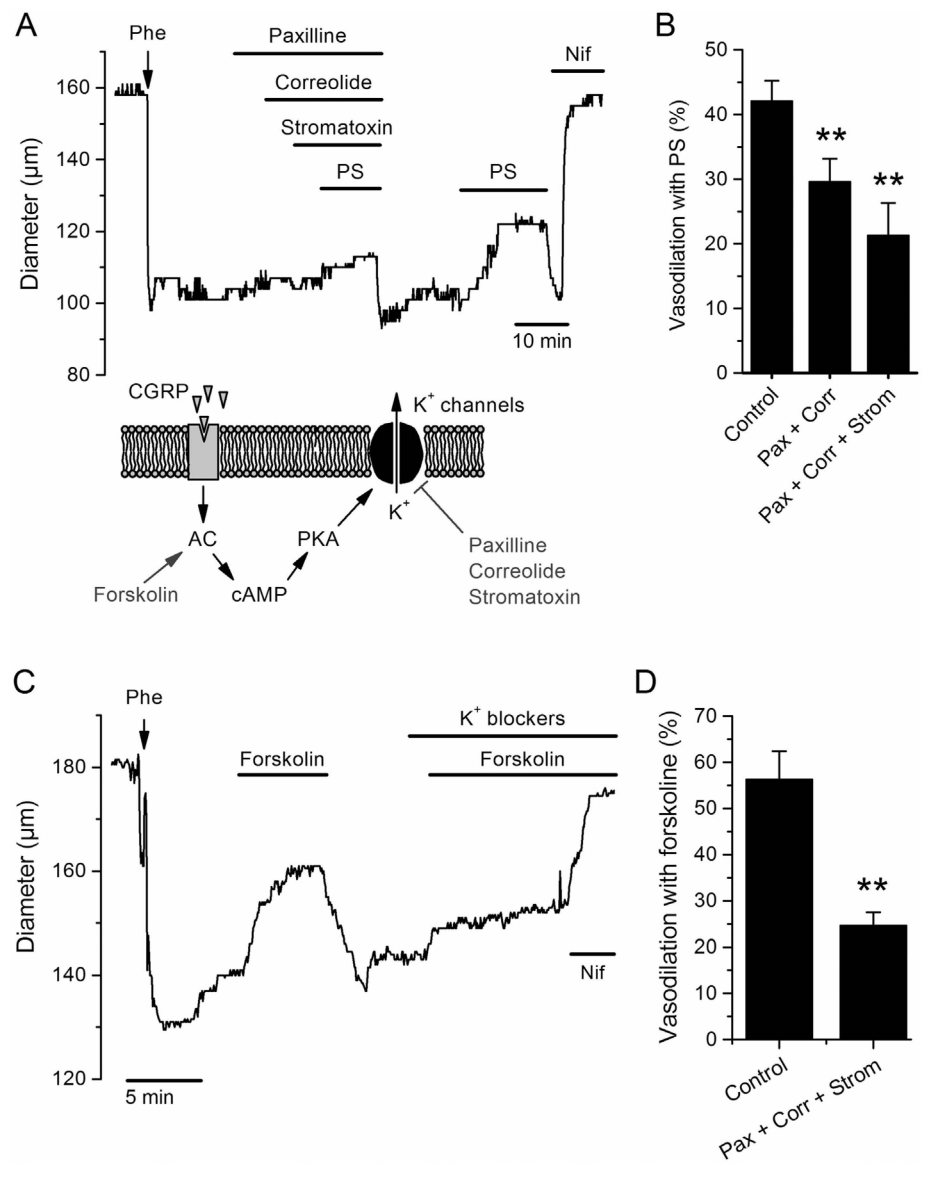
A
Phe
Paxilline
Correolide
Stromatoxin
PS
PS
Nif
10 min
Diameter (µm)
160
140
120
100
80
CGRP
K+ channels
AC
PKA
K+
Forskolin
cAMP
Paxilline
Correolide
Stromatoxin
B
Vasodilation with PS (%)
50
40
30
20
10
0
**
**
Control
Pax + Corr
Pax + Corr + Strom
C
Phe
K+ blockers
Forskolin
Forskolin
Nif
5 min
Diameter (µm)
180
160
140
120
D
Vasodilation with forskoline (%)
70
60
50
40
30
20
10
0
**
Control
Pax + Corr + Strom

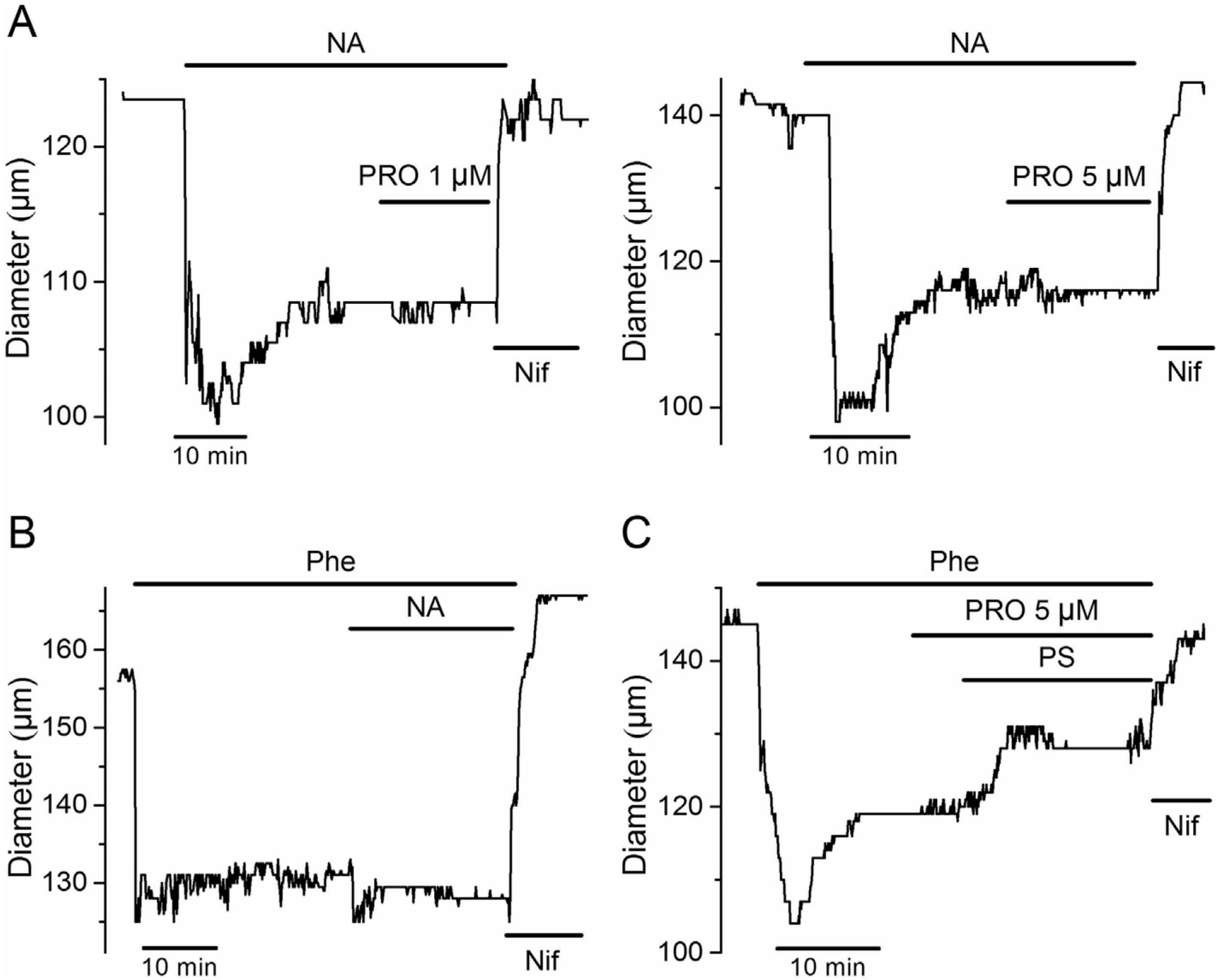
A
NA
PRO 1 µM
Nif
Diameter (µm)
120
110
100
10 min
NA
PRO 5 µM
Nif
140
120
100
10 min
B
Phe
NA
Nif
160
150
140
130
10 min
C
Phe
PRO 5 µM
PS
Nif
140
120
100
10 min

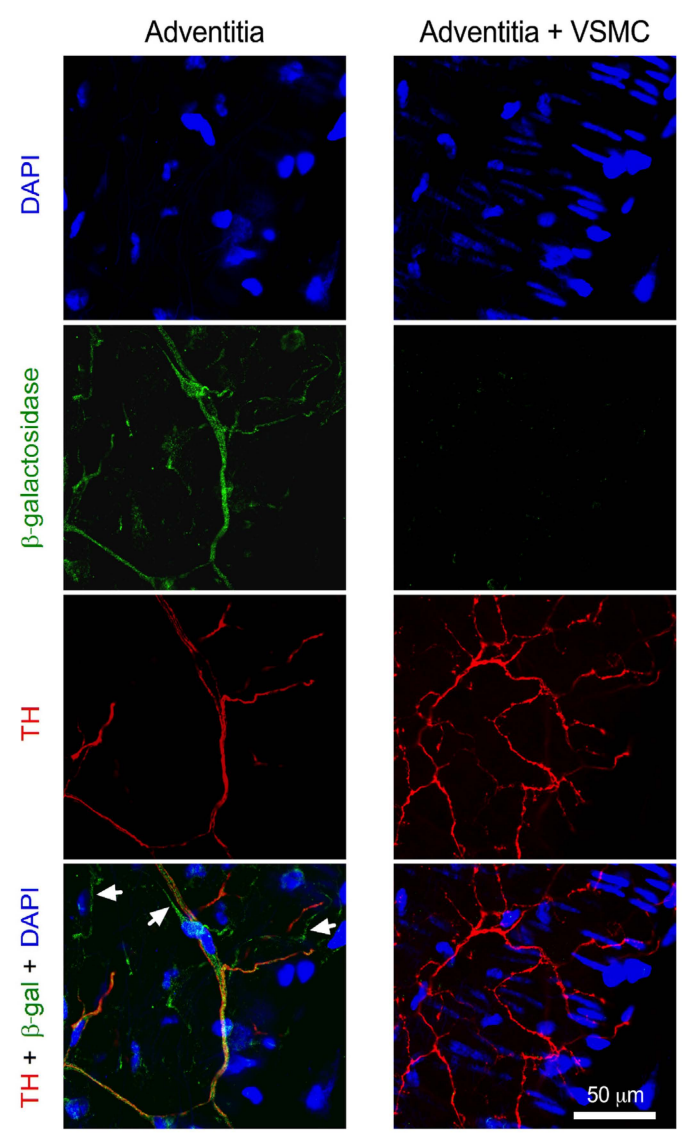
Adventitia
Adventitia + VSMC
DAPI
β-galactosidase
TH
TH + β-gal + DAPI
50 μm

SUPPLEMENTAL FIGURES

Activation of the cation channel TRPM3 in perivascular nerves induces vasodilation of resistance arteries

Lucía Alonso-Carbajo[1,2], Yeranddy A. Alpizar[1], Justyna B. Startek[1], José Ramón López-López[2], María Teresa Pérez-García[2] and Karel Talavera[1]

[1] Department of Cellular and Molecular Medicine, Laboratory of Ion Channel Research, KU Leuven; VIB Center for Brain & Disease Research, Herestraat 49, Campus Gasthuisberg, O&N1 Box 802, 3000 Leuven, Belgium.

[2] Departamento de Bioquímica y Biología Molecular y Fisiología, Instituto de Biología y Genética Molecular, Universidad de Valladolid y CSIC, Sanz y Forés 3, 47003 Valladolid, Spain.

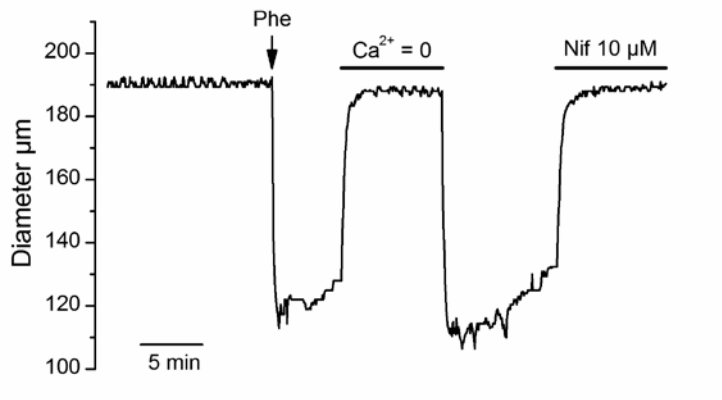

Supplementary Fig. 1. Nifedipine (10 µM) induces maximal vasodilation in mouse mesenteric arteries. Comparison of the vasodilating effects of a Ca^{2+}-free solution and 10 µM nifedipine (Nif) in WT arteries. Phenylephrine is defined as Phe.

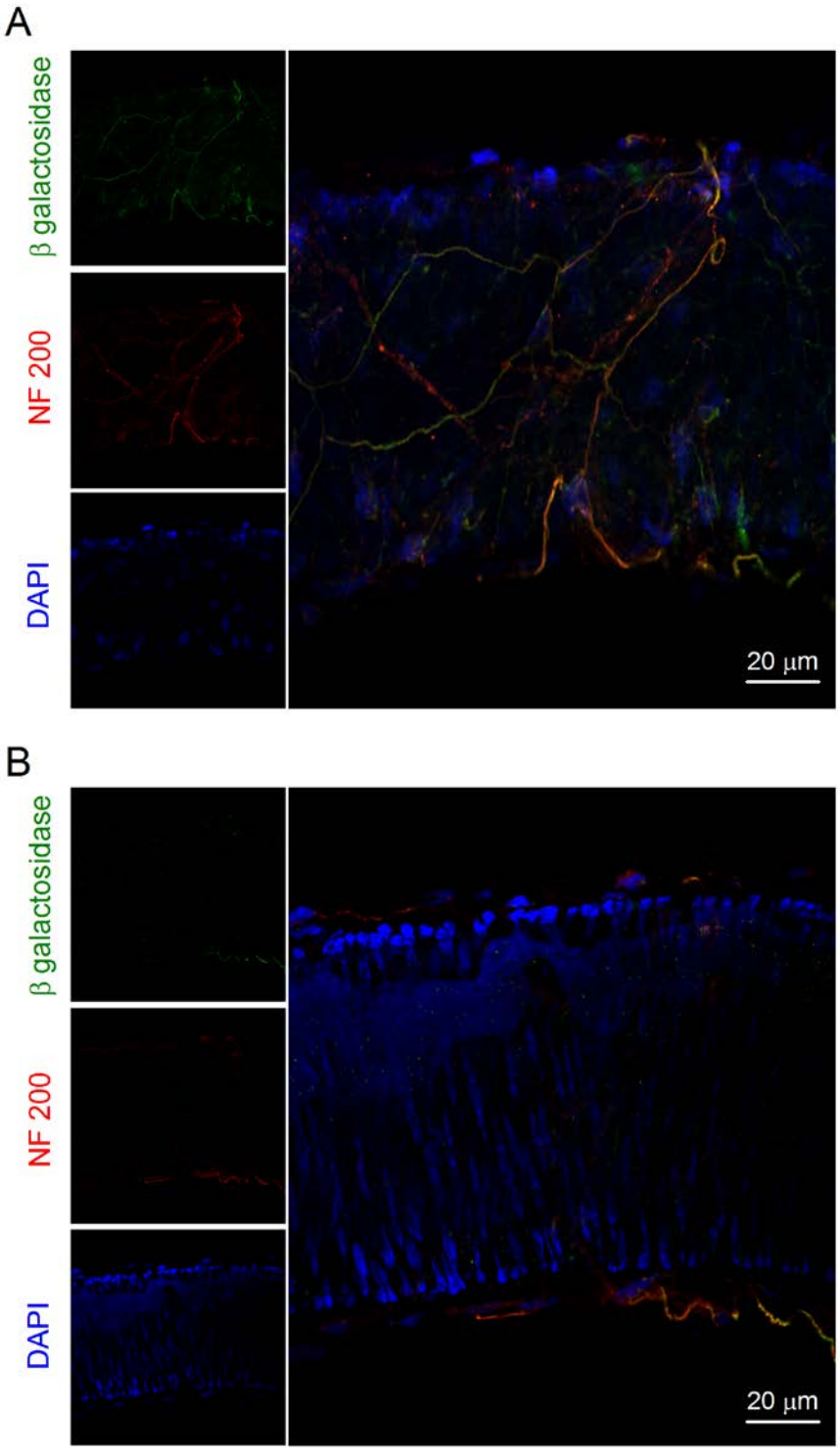

Supplementary Fig. 2. Perivascular innervation in dissected mouse mesenteric arteries. Confocal images of the adventitia (*A*) and the medial layer (*B*) of intact *Trpm3* KO mesenteric arteries labeled with β galactosidase (green), anti-NF-200 (red) antibodies and nuclear DAPI (blue) staining. Images are representative of at least 3 independent experiments.

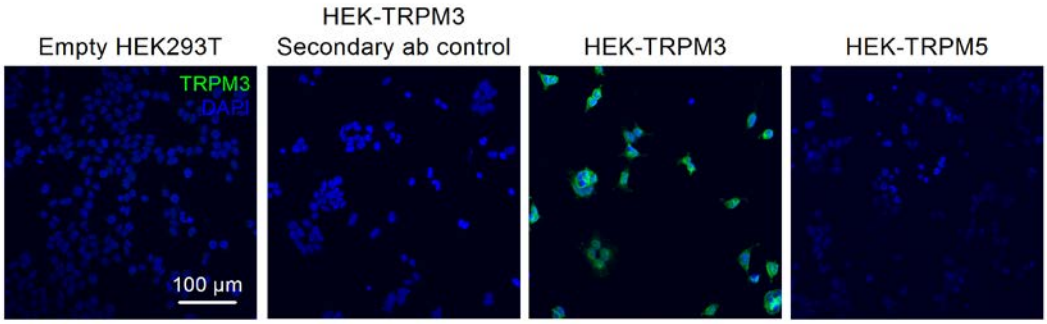

Supplementary Fig. 3. Specificity of a rabbit anti-TRPM3 antibody. Confocal images of non-transfected cells incubated with the anti-TRPM3 antibody, non-transfected cells incubated with the secondary antibody, TRPM3-transfected cells labeled with the anti-TRPM3 antibody and TRPM5-transfected cells incubated with anti-TRPM3. In all images DAPI staining is shown in blue. Images are representative of at least 3 independent experiments.

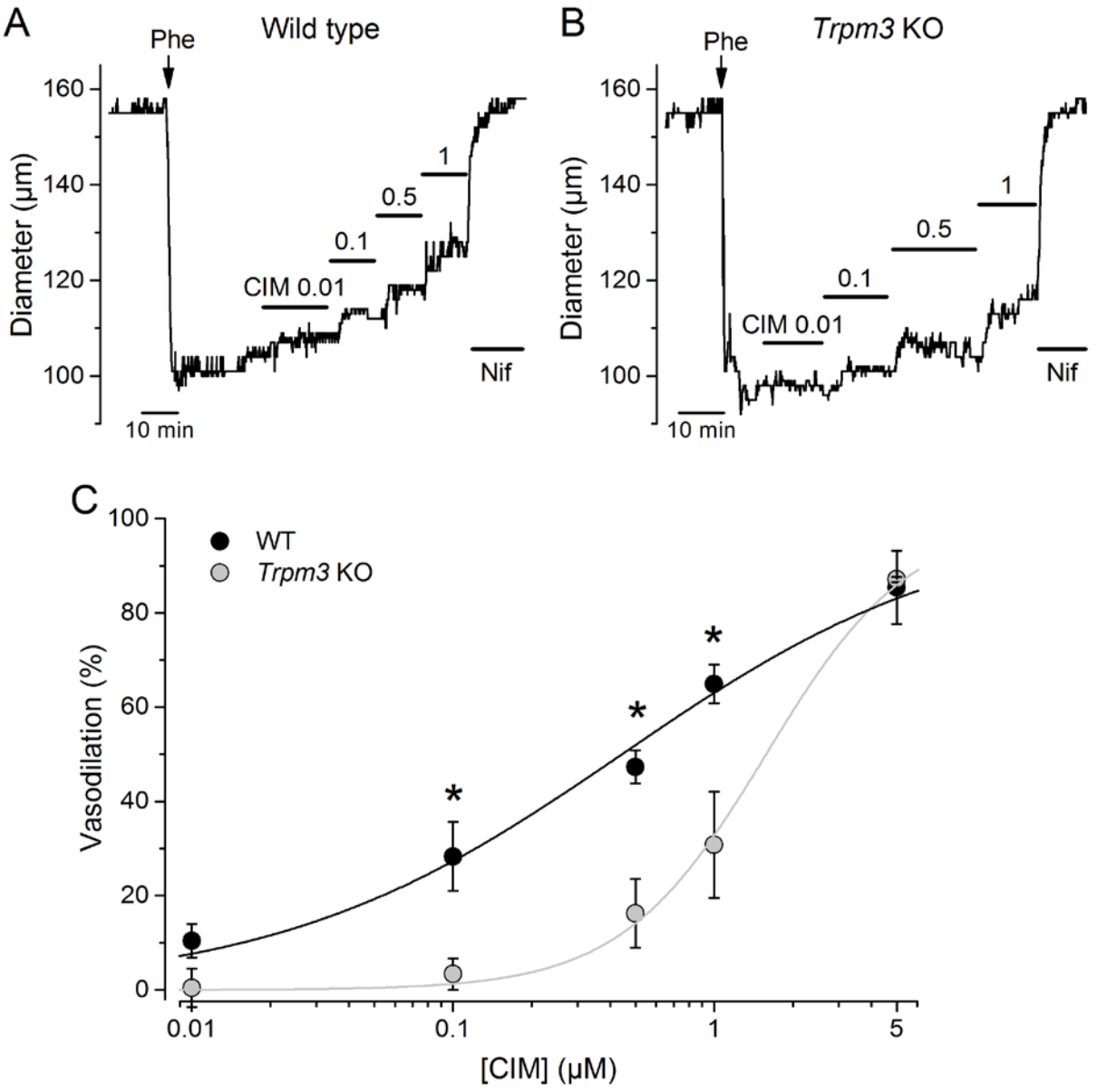

Supplementary Fig. 4. A synthetic potent agonist of TRPM3 induces vasodilation of endothelium-denuded mesenteric arteries. Representative examples of the effects of CIM0216 at different concentrations applied on the diameter of arteries dissected from WT (*A*) and *Trpm3* KO mice (*B*). (*C*). Dose dependency of CIM0216-induced vasodilation in arteries dissected from WT and *Trpm3* KO mice. Nifedipine (Nif, 10 µM) was applied at the end of each experiment. Data is obtained from the average of 4 arteries from 4 different WT mice and 4 arteries from 4 different *Trpm3* KO mice. Phe = Phenylephrine. **P* < 0.05 compared to WT mice, paired t-test.

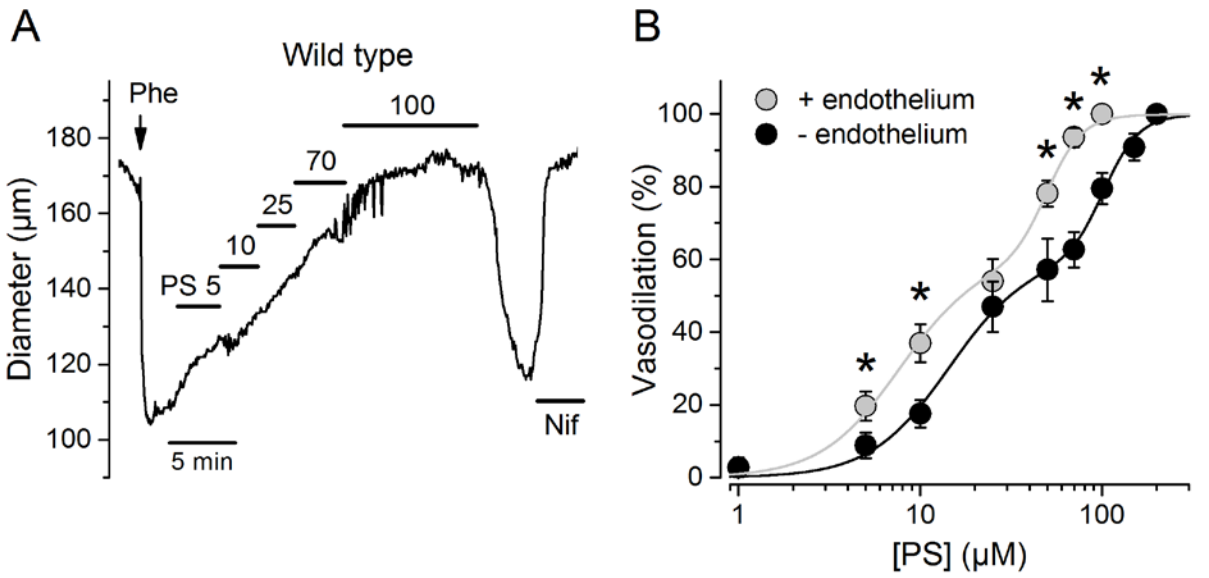

Supplementary Fig. 5. TRPM3-induced vasodilation of mesenteric arteries is enhanced by endothelium. *(A)* Representative example of the vasodilation induced by PS in a WT mouse mesenteric artery with endothelium precontrated with phenylephrine (10 µM). At the end of each experiment, Nif (10 µM) was applied. (*B*) Comparison of the dose responses to PS in precontrated arteries with endothelium (n = 8 arteries from 6 animals) and without endothelium (n = 10 arteries from 7 animals, same data as in *Figure 5D* is shown for comparison). The solid lines represent the best fit of the data with two-component Hill equations. * indicates $P < 0.05$ compared to the corresponding data for WT without endothelium, unpaired t-test.

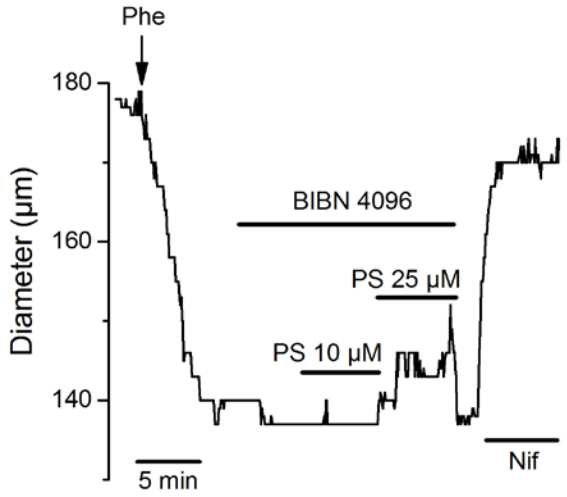

Supplementary Fig. 6. PS (10 µM) does not induce vasodilation in the absence of CGRP signaling. Effects of PS (10 µM and 25 µM) on a WT mouse mesenteric artery in the presence of the CGRP receptor antagonist BIBN 4096. Phe = Phenylephrine, PS = pregnenolone sulfate and Nif = nifedipine.

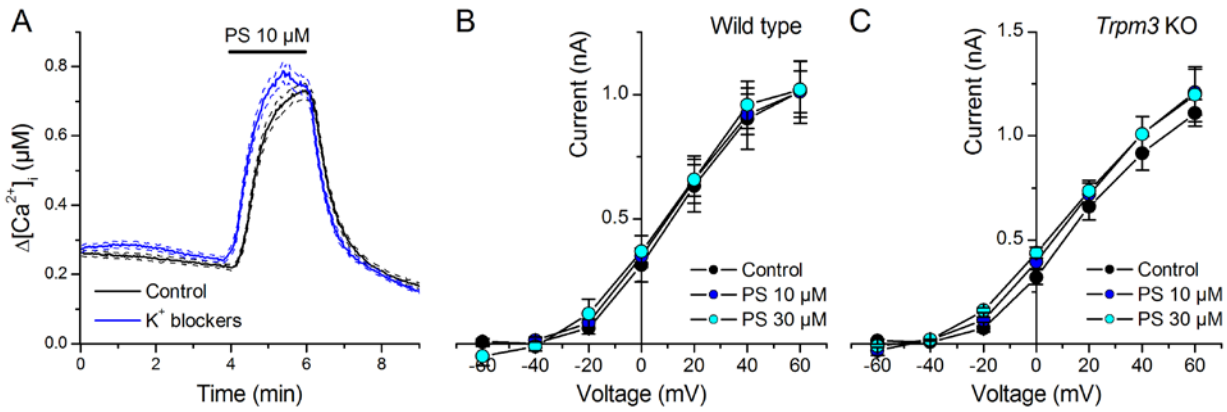

Supplementary Fig. 7. Absence of non-specific effects of K^+ channel blockers on TRPM3 channels or PS on K^+ channels (A) Intracellular Ca^{2+} signals in HEK293T-TRPM3 cells stimulated with 10 µM PS in control (n = 25) was not affected by the presence of a cocktail of K^+ channel blockers including paxilline, correolide and stromatoxin (n = 25). Voltage-dependence of the amplitude of K^+ currents recorded VSMC isolated from WT (*B*) and *Trpm3* KO (*C*) mice in control and in the presence of 10 or 30 µM PS (n = 10 cells from 4-6 mice).